Food Chemistry 479 (2025) 143753

Contents lists available at ScienceDirect

Food Chemistry

journal homepage: www.elsevier.com/locate/foodchem

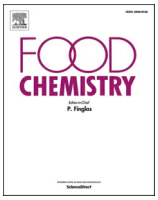

Metabolite variations in faba bean ingredients: Unraveling the links between off-flavors and chemical compounds

Fabio Tuccillo [a,*], Anna Kårlund [b], Ville Koistinen [b,c], Shania Saini [b], Hany Ahmed [b], Kati Hanhineva [b,c], Mari Sandell [a,d], Kati Katina [a], Anna-Maija Lampi [a]

[a] Department of Food and Nutrition Sciences, University of Helsinki, Helsinki, Finland
[b] Food Sciences Unit, Department of Life Technologies, University of Turku, Turku, Finland
[c] Institute of Public Health and Clinical Nutrition, School of Medicine, Faculty of Health Sciences, University of Eastern Finland, Kuopio, Finland
[d] Nutrition and Food Research Center, University of Turku, Turku, Finland

ARTICLE INFO

Keywords:
Vicia faba
Metabolomics
Sensory
Bitterness
Pulses
Broad bean
Protein

ABSTRACT

Faba bean ingredients are attracting interest for their suitability in producing protein-rich plant-based foods. However, their sensory characteristics (e.g., bitterness) challenge consumer acceptance. This study explored variations in the metabolome and the links between metabolites and sensory attributes using UHPLC-qTOF-MS/MS analysis of faba bean flour, two protein concentrates, and protein isolate. Partial Least Squares regression identified metabolites contributing to sensory descriptors, and it was validated against the VirtuousMultiTaste platform. Genetic variation and processing methods contributed to the metabolite composition of faba bean ingredients. We annotated 115 compounds with choline and vicine having the highest relative abundance. Five clusters suggested cultivar-specificity and process-related differences. Several compounds were linked to bitterness and mouth-drying orosensation, including caprolactam, gingerglycolipid, lysine, and vicine. Some compounds were reported as potentially bitter for the first time. This study lays the foundation for further research on the bitterness of these compounds and receptor-level investigations for targeted flavor optimization.

1. Introduction

Faba beans (*Vicia faba* L.) have garnered increasing attention in agricultural and food science due to their nutritional value and their potential to improve the sustainability of food systems (Augustin & Cole, 2022). Given their high yields and ability to fix nitrogen, faba beans could address the dietary requirements of a growing population, which has shown interest in more sustainable plant-based diets (Foyer et al., 2016; Medawar et al., 2019). While faba beans can also thrive in colder climates, they have a rich history of traditional consumption in the Mediterranean and West Asian regions (Flores et al., 2013; Inci & Toker, 2011; Pasqualone et al., 2020). In addition, the versatility of faba beans enables the production of ingredients such as flour, protein concentrate, and protein isolate, which can be utilized in various food products, including pasta, bread, and dairy and meat alternatives (Dhull et al., 2021). Despite their potential, the sensory characteristics of faba bean ingredients pose a challenge to widespread consumer acceptance (Wang et al., 2022). Specifically, the bitter taste of these ingredients acts as a warning signal (Spaggiari et al., 2020) and was found to be the main reason for consumers' dislike of these ingredients (Tuccillo et al., 2024).

Off-flavors, defined as unpleasant taste, odor, and chemesthetic characteristics, can significantly impact the palatability and consumer appeal of food products (Menis-Henrique, 2020). In the case of faba bean ingredients, differences in off-flavors can be attributed to various factors, including genetic variability among cultivars, environmental influences during cultivation, alongside processing and storage conditions (Akkad et al., 2019, Akkad et al., 2021, Akkad et al., 2022). Currently, the variation and availability of commercial faba bean ingredients are limited, especially compared to pea and soy (Business Intelligence Consulting, 2023). This scarcity acts as a barrier for the industry, often necessitating strategies such as the addition of salt, spices, and e-coded flavorings in food production processes (Roland et al., 2017). While this has led researchers to investigate the factors contributing to off-flavors in faba bean-based products, little is known about the possible off-flavors causing compounds (Karolkowski et al., 2022; Karolkowski, Belloir, Lucchi, et al., 2023; Tuccillo, Kantanen, et al., 2022; Tuccillo, Wang, et al., 2022; Wang et al., 2024). Identifying the potential compounds responsible for off-flavors can enable the implementation of

* Corresponding author at: Department of Food and Nutrition Sciences, University of Helsinki, P.O. Box 66 (Agnes Sjöbergin katu 2), FI-00014, Helsinki, Finland.
E-mail address: fabio.tuccillo@helsinki.fi (F. Tuccillo).

https://doi.org/10.1016/j.foodchem.2025.143753
Received 5 December 2024; Received in revised form 17 February 2025; Accepted 4 March 2025
Available online 12 March 2025

more sustainable practices, such as bioprocessing and fermentation, to reduce the concentration of such compounds and improve the overall sensory perception (Wang et al., 2022).

Metabolomics involves the analysis of small (<1500 Da) molecular metabolites or chemicals in biological samples which helps in identifying flavor compounds and understanding the mechanisms of their formation (Wishart, 2008). It also allows for quality control, early detection of off-flavors, and optimization of flavor profiles in food products (Cevallos-Cevallos et al., 2009). Liquid chromatography coupled with mass spectrometry (LC–MS) techniques are commonly employed in metabolomics analyses of non-volatile flavor compounds ascribed to their high sensitivity, specificity, and ability to detect large portions of the metabolome (Klåvus et al., 2020; Wishart, 2008). This makes metabolomics particularly valuable in addressing flavor-related challenges, especially considering the multitude of bitter compounds present in nature (Spaggiari et al., 2020). In addition, predictive models using sample metabolite profiles facilitate the flavor optimization of faba bean ingredients (Cevallos-Cevallos et al., 2009). Despite the importance of metabolites in flavor development, there has been limited research on the differences in metabolite profiles among different faba bean ingredients, although this approach has been adopted for other pulses (He et al., 2023; Shiga et al., 2014).

The aim of this study was to (I) assess the overall variation in the metabolome of a faba bean flour, two protein concentrates, and a protein isolate, (II) highlight differences in the abundance of possible sensory-relevant non-volatile metabolites among the ingredients, and (III) identify potential non-volatile off-flavor compounds using multivariate methods. Our results contribute to the understanding of the underlying molecular aspects behind the off flavors of faba bean ingredients and provide a basis for future investigations in isolated forms as well as at the receptor level. Ultimately, our findings will advise future studies on off-flavor mitigation strategies, potentially guiding the development of targeted processing techniques or interventions at the molecular level to enhance the sensory quality of faba bean ingredients.

2. Materials and methods

2.1. Faba bean ingredients

Four commercially available faba bean ingredients from two manufacturers and two cultivar selections were used in this study. Faba bean flour (FF) and faba bean protein concentrate b (FPCb) (cultivar Kontu) were purchased from Suomen Viljava Oy© (Helsinki, Finland), whereas faba bean protein isolate (FPI) and faba bean protein concentrate a (FPCa) (cultivars Snowbird, Tabasco, Malik, FBP-4) were purchased from AGT Food and Ingredients© (Regina, SK, Canada). The ingredients used in this study were the same as those employed in two previous studies, as described next. In the first study (Tuccillo, Kantanen, et al., 2022), faba bean ingredients and their blends were processed into extrudates using high-moisture extrusion, and their sensory profiles were characterized. In addition, the materials were analyzed for proximate composition, lipase and lipoxygenase activities, volatile compounds, flavor precursors, total free phenolics, total condensed tannins, soyasaponins B and βG, vicine, and convicine. In the second study (Tuccillo et al., 2024), 265 participants evaluated their liking for smell, taste, overall liking, and willingness to use these ingredients prepared as minimally processed pastes in water.

2.2. Sensory profiling

The sensory profiles of the faba bean ingredients from our previous research (Tuccillo, Kantanen, et al., 2022) was generated using Generic Descriptive Analysis, and the data were used in the regression models of the present study. A trained panel ($N = 10$, 8 females) was recruited from the Department of Food and Nutrition at the University of Helsinki based on prior experience with sensory profiling of similar plant-based samples. All participants provided written informed consent to voluntarily participate in this study, which was approved by the University of Helsinki Ethical Review Board in Humanities and Social and Behavioral Sciences (Statement 15/2020).

The entire study was conducted in a sensory laboratory following ISO 8589 standards. Panelists participated in three training sessions (1–2 h per session), during which they agreed on the lexicon, descriptions, and the type and intensity of reference samples. Training also covered the use of the scale, and panel performance was monitored using 3-way analysis of variance (ANOVA) and principal component analysis (PCA). Both English and Finnish were used during training and evaluation sessions.

Each evaluation session consisted of eight samples: four ingredients described in Section 2.1 and four blends. All samples were prepared as suspensions in tap water at a 1:3 (*w*/w) ratio, thoroughly mixed, and served (10 g) in plastic cups with lids labeled with three-digit codes at room temperature. Samples were presented in a randomized block design across sessions and assessors.

Panelists were instructed to assess the intensity of each attribute by comparing the samples to a reference sample. Intensity was rated on a 0–10 line scale, with 0 representing “not at all” and 10 representing “very strong.” To cleanse their palate between samples, panelists drank water, chewed a puffed corn snack, and took a short break. Evaluations were conducted in triplicate under white light with controlled air conditioning. Data were collected using RedJade© software (RedJade Sensory Solutions LLC, Boulder, CO, USA).

2.3. Sample preparation for UHPLC-qTOF-MS analysis

For non-targeted metabolomic analysis, 100 mg of each sample was extracted in 500 μL of cold 80 % methanol (Fluka Honeywell, Charlotte, NC, USA) in ultrapure water (Elga, Veolia Water Solutions and Technologies, Woodridge, IL, USA) by vortexing for 5 min at room temperature. Then, the samples were centrifuged at 10,000 ×*g* for 2 min at 4 °C. An aliquot of 200 μL was diluted with 800 μL 80 % methanol in ultrapure water and centrifuged at 10,000 ×*g* for 10 min at 4 °C. The supernatant was filtered through a Pall Acrodisc 13 mm syringe filter with a 0.2 μm PTFE membrane (Thermo Fisher Scientific, Pittsburgh, PA, USA), and 250 μL of the filtrate was transferred into an LC-MS vial with an insert. Three analytical replicates were used for each sample. In addition, a quality control (QC) sample was prepared by combining 20 μL of each replicate sample, and a blank sample containing 80 % methanol in ultrapure water was prepared by following the same sample treatment. While methanol effectively extracts polar metabolites, its limitation is the poor extraction of non-polar compounds, which may result in a partial metabolite profile.

2.4. UHPLC-qTOF-MS analysis

Non-targeted metabolomics analysis was performed using a UHPLC-qTOF-MS system (Agilent Technologies, Waldbronn, Karlsrue, Germany) consisting of an Infinity 1290 II LC system coupled to a 6546 UHD accurate-mass qTOF spectrometer with Jetstream electrospray ionization (ESI) in both positive (+) and negative (−) modes (Klåvus et al., 2020). The sample sequence was randomized, and prior to sample injections, solvent blanks were injected at the beginning of the sequence followed by ten QC injections for system equilibration. QC samples were injected after every six sample injections. The temperature of the sample tray was set at 4 °C. Additionally, data-dependent product ion scans (MS/MS) using collision energies of 10, 20, and 40 eV were acquired for each mode at the beginning and end of the sequence from QC samples.

Both Hydrophilic Interaction Liquid Chromatography (HILIC) and Reversed Phase (RP) chromatographic separation techniques were utilized. Separation of hydrophilic metabolites was performed using a HILIC column (Acquity UPLC BEH Amide 1.7 μm, 2.1 × 100 mm, Waters, Ireland). The column oven temperature was set at 45 °C, with a flow rate

of 600 μL/min for the gradient profile, using 50 % (*v*/v) acetonitrile (Riedel-de Haën™, Honeywell, Seelze, Germany) in water (eluent A) and 90 % (v/v) acetonitrile in ultrapure water (eluent B), both containing 20 mM ammonium formate (pH 3) (LiChropur™, Supelco, Merck, Darmstadt, Germany). The gradient profile was 0–10 min: 2 % B → 100 % B; 10–14.5 min: 100 % B; 14.5–14.51 min: 100 % B → 2 % B; 14.51–16.5 min: 2 % B. Separation of the amphiphilic metabolites was performed using an RP column (Zorbax Eclipse XDB-C18 1.8 μm, 2.1 × 100 mm, Agilent Technologies, USA). The column oven temperature was set at 50 °C with a flow rate of 400 μL/min for the gradient profile with water (eluent A, ultra-pure water) and methanol (eluent B, Riedel-de Haën™, Honeywell, Seelze, Germany), both containing 0.1 % (v/v) formic acid (HiPerSolv Chromanorm™, VWR, Leuven, Belgium). The gradient was 0–10 min: 2 % B → 100 % B; 10–14.5 min: 100 % B; 14.5–14.51 min: 100 % B → 2 % B; 14.51–16.5 min: 2 % B. An injection volume of 2 μL was used across the analysis.

The instrument was operated using MassHunter Workstation Data Acquisition v. 11.0 (Agilent Technologies), and instrument parameters in the full scan mode were set to high-resolution (10 GHz) mode, with a mass range of 50–1600 *m/z*, abundance threshold of 150, and scan time of 1.67 Hz. The source parameters for all analyses were set as follows: drying gas flow, 10 L/min; temperature, 325 °C; sheath gas flow, 11 L/min; temperature, 350 °C; nebulizer pressure, 45 psi; capillary voltage, 3500 V; and nozzle voltage, 1000 V. Additionally, specific parameters for the MS/MS analyses were an abundance threshold of 200, target of 25,000 counts/spectrum, scan time of 3.33 Hz, maximum of 4 precursors per cycle, precursor isolation width of 1.3 Da, active exclusion after 2 spectra, and release after 0.25 min. The detector was calibrated prior to the sample sequences, and continuous mass axis calibration was applied by monitoring the reference ions, m/z 121.050873 and m/z 922.009798 in the positive mode alongside m/z 112.985587 and m/z 1033.988109 in the negative mode, for high (< 2 ppm) mass accuracy.

2.5. Data processing

The *notame* analytical workflow (Klåvus et al., 2020) was used in this study for non-targeted metabolic profiling. For peak picking and alignment, we utilized the MS-DIAL (RIKEN PRIMe, Japan) software v. 4.9.221218, with specific parameters. Peaks were picked within a retention time range of 0–100 min, and the MS and MS/MS mass ranges were set from 0 to 2000 Da. The MS1 tolerance was set to 0.01 Da, and the MS2 tolerance was set to 0.025 Da. We used a maximum charge of two for isotope recognition, and data processing was conducted using a single thread. The peak detection parameters included the Linear Weighted Moving Average smoothing method, with a smoothing level of 3. Additionally, a minimum peak width of 5 Da and minimum peak height amplitude of 2000 were applied as filters. For peak alignment, a QC sample from the middle of the sequence was used as a reference, with a retention time tolerance of 0.05 min for RP and 0.3 min for HILIC, apart from an MS1 tolerance of 0.051 Da. Drift correction and flagging of low-quality features were performed using Posit (formerly R Studio v. 4.2.2, Massachusetts, US) and the *notame* package (https://github.com/antonvsdata/notame). Molecular features exhibiting a detection rate below the recommended threshold of 70 % in the QC samples and molecular features with relative standard deviation (RSD) > 0.2 and D-ratio > 0.4 were flagged as low QC detection features and low-quality features. Moreover, the features were filtered based on their quality and relevance to the study aim. Table 1 provides an overview of the quality (QF), and relevance filters (RF) applied to the metabolomic data along with the number of features retained after each filter. The filters applied were flagging based on QC samples, absence in blank samples, signal-to-noise ratio (S/N) greater than 5, availability of MS/MS data, a 2Log fold change cutoff of < −2 and > 2 in at least one pairwise comparison between the sample types, a *p*-value threshold of 0.01 from ANOVA, and a Variable Importance in Projection (VIP) score greater than 1. Detailed descriptions of the criteria and statistical methodologies employed for each RF can be found in Section 2.7.

Table 1
Overview of quality (QF) and relevance filters (RF) applied to the metabolomic data and number of features retained.

filter applied	number of features	filter type
no filters	41,151	n/a
low-QC-detection and low-quality features	26,465	QF
absence in blank sample	7344	QF
$S/N > 5$	34,690	QF
MS/MS available	2439	QF
2Log fold change < −2 and > 2	33,197	RF
ANOVA, *p-value* < 0.01	32,307	RF
VIP* > 1	25,994	RF
all QF filters applied	239	QF
all RF filters applied	19,609	RF
both QF and RF filters applied	122	QF and RF

QC, Quality Control; S/N, Signal-to-Noise ratio; ANOVA, Analysis of Variance; VIP, Variable Importance in Projection; * VIP calculated from a Partial Least Squares regression model having all detected features (n = 41,151) as predictors and previously reported (Tuccillo, Kantanen, et al., 2022) sensory profile data as responses.

2.6. Metabolite annotation

First, the detected features were annotated semi-automatically using internal libraries imported into MS-DIAL. Separate libraries for positive and negative modes, including ESI(+) and ESI(−) MS/MS spectra from in-house standards, biological sources, and in silico sources were utilized, which were sourced from the MS-DIAL metabolomics MSP resource (RIKEN PRIMe, Japan). For peak matching, exact *m/z*, retention time, and MS/MS spectra were chosen. The accurate mass tolerances for MS1 and MS2 were set to 0.01 Da and 0.05 Da, respectively. The identification score cutoff was set to an 80 % similarity score.

Second, the annotation of retained features after applying QF and RF was manually curated using the spectral databases and published literature. This curation involved matching the observed data, especially MS/MS fragmentation pattern, with the database entries. MS-DIAL and Agilent MassHunter Qualitative Analysis 10.0 software were used to explore the MS and MS/MS data. The compound ontology was confirmed using Classyfire database (Djoumbou Feunang et al., 2016). The levels of identification and annotation in this study comprised the following categories: Level 1, compounds that were identified using in-house chemical standards; Level 2, compounds that were identified through MS/MS data matching against public databases or standards in the absence of MS/MS information; Level 3, compounds that were characterized based on their chemical class or sub class using physico-chemical information; and Level 4, compounds for which identification could not be determined (Sumner et al., 2007). Unknown compounds, or compounds for which only the class is known, are reported with the observed monoisotopic mass and retention time (e.g., Unknown 374.1418_2.177). In cases where the same compound was annotated in both positive and negative ionization modes, or from both HILIC and RP chromatographic methods, the mode with most abundant base peak signal was reported.

2.7. Metabolomics data analysis and feature selection

Quality control of the raw data, encompassing metabolomic features from all chromatographic types, electrospray ionization polarities, and samples (including QC and blank), was conducted using Posit and the *notame* package. It consists of RSD, D-ratio (Fig. S1), and hierarchical cluster analysis (HCA) performed using the Ward method and Euclidean distance as the proximity measure (Fig. S2). Total ion chromatograms (Fig. S3) were inspected. Averages, standard deviations, and 2Log fold changes of peak areas were calculated for each feature of the raw data (excluding QC and blank samples) using Microsoft Excel v. 2308. The

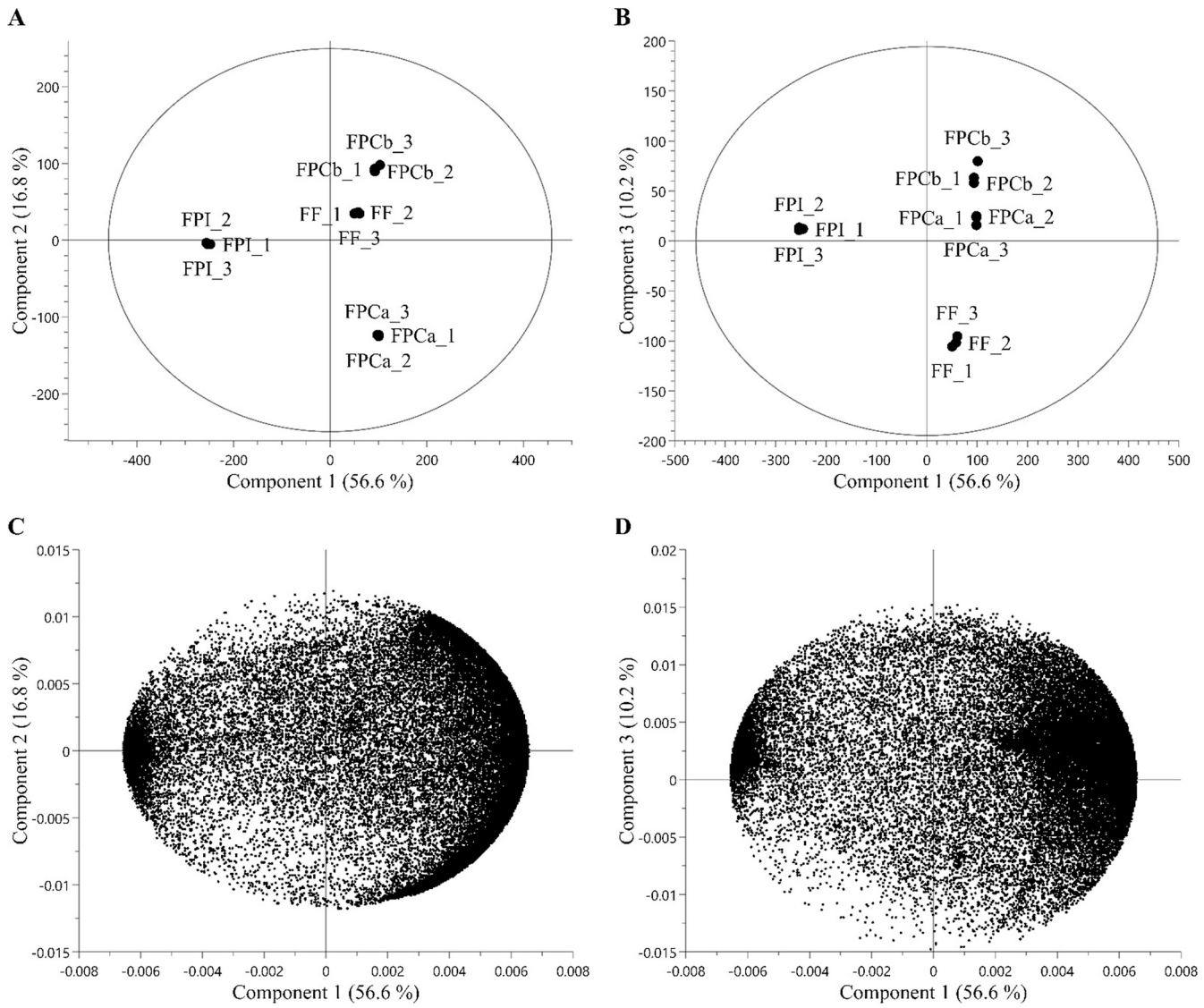

Fig. 1. Principal Component Analysis (PCA) scores (A, B) and loading plots (C, D) of detected features (N = 41,151) in faba bean samples (three replicates, N = 12), namely faba bean flour (FF), faba bean protein concentrates (FPCa, FPCb), and faba bean protein isolate (FPI). The scores and loadings are shown along the first and second components (A, C) and the first and third components (B, D).

2Log fold change for each sample pair was determined based on three measurements of peak area values. Features were retained if at least one pair exhibited a 2Log fold change of < -2 and > 2. Furthermore, 1-way ANOVA was carried out with Posit to evaluate the statistical differences among the peak areas of each feature across the four samples over the three measurements. Additionally, Partial Least Squares Regression (PLS) analysis was performed using SIMCA v. 17.0.2 (Sartorius Corporate Administration, Göttingen, Germany) to select features for further annotation based on their Variable Importance in Projection (VIP) scores in relation to sensory attributes. This analysis involved 41,164 variables, with 41,151 representing the predictive variables (features) and 13 representing the response variables (sensory attributes) reported elsewhere (Tuccillo, Kantanen, et al., 2022). The average values of the peak areas were used for the analysis, and the data was mean-centered and UV-scaled. Cross-validation of the model was performed. Furthermore, PCA was performed to visually explore the differences in the metabolome among the samples, including replicates ($N = 12$). Herein, PCA was carried out using SIMCA, using the peak areas of all detected features ($N = 41,151$), after mean-centering and UV-scaling. Cross-validation was applied to the model.

2.8. Statistical analysis of annotated features

Subsequent statistical analyses were performed on the annotated features ($N = 115$), which remained after implementing QF, RF, and duplicate entry removal. These features included both compounds for which suggestions for identification were made and those that remained unknown. To obtain a broad overview of this dataset, we plotted the annotated features by retention time and *m/z*, sized them by log-transformed average peak area across replicates and samples, and shape- and color-coded them based on the separation mode and compound class. To observe differences in the compound classes, the relative abundances of compound classes across all features for each sample were computed. To find clustering patterns across samples and features, HCA based on the Ward method and Euclidean distance, and a heatmap were computed in Posit using the *Pheatmap* package (https://cran.r-project.org/web/packages/pheatmap/index.html). The color scale in the heat map reflects the peak areas after scaling. To pinpoint differentiating metabolites, volcano plots comparing the metabolite profiles of FPCa vs. FPCb (same process, different origin), FPCa vs. FPI (different process, same origin), and FPCb vs. FF (different process, same origin) were computed. The x-axis, representing fold change, was converted to a

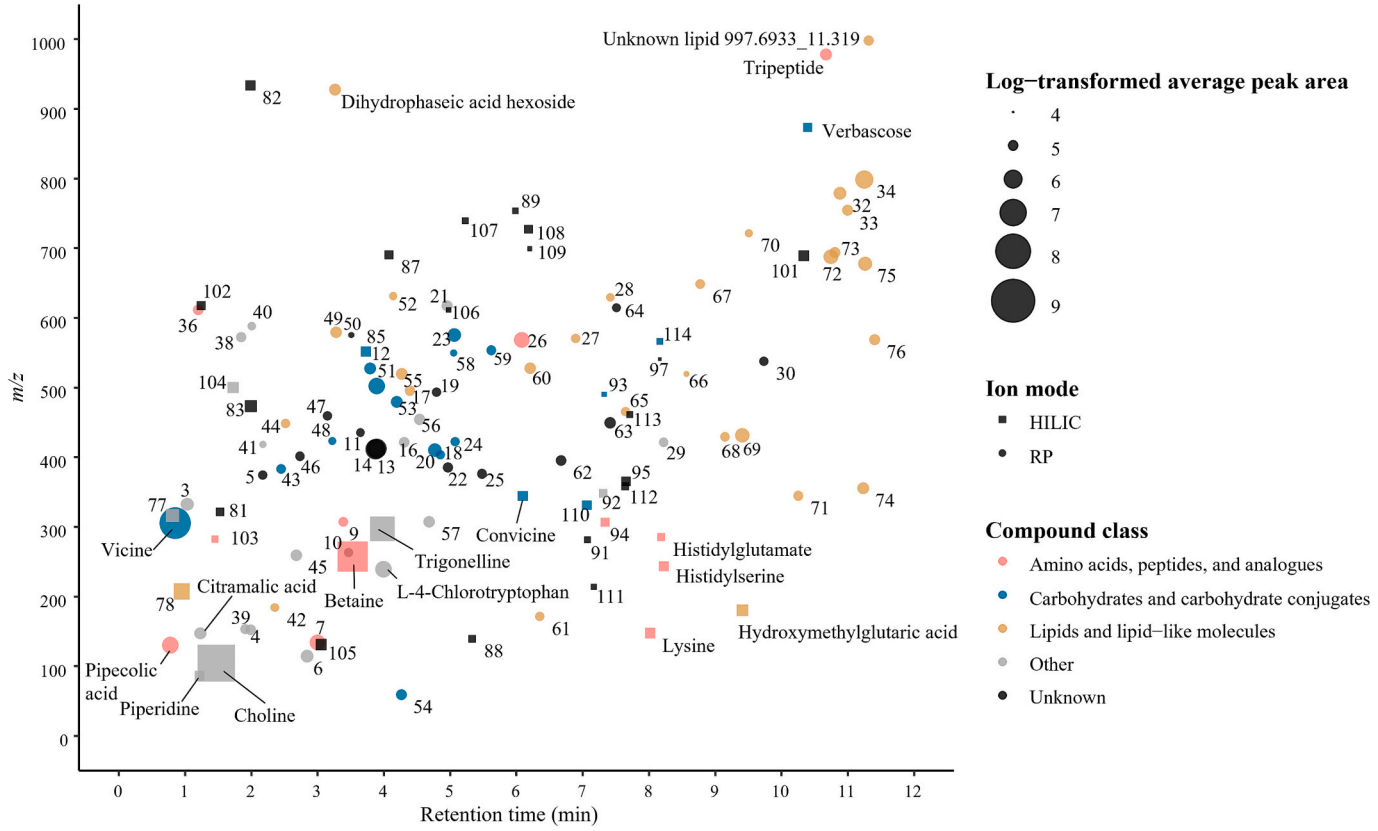

Fig. 2. Annotated metabolites ($N = 115$) plotted against retention time (min) and *m/z* (mass-to-charge ratio). The dot size reflects the log-transformed average peak area across the samples, shapes denote the separation mode (HILIC: Hydrophilic Interaction Liquid Chromatography - squares, RP: Reverse Phase - circles), and colors represent compound classes. Table A1 lists the compound names corresponding to each metabolite's ID.

positive logarithmic scale base-2, while the y-axis, indicating the *p*-value, was converted to a negative logarithmic scale base-10. To link the annotated features (predictors) to the previously reported (Tuccillo, Kantanen, et al., 2022) sensory attributes (responses), a PLS model was computed using The Unscrambler® X (v. 10.5, Camo Software, Oslo, Norway). In the model, the average peak areas of the annotated features across the samples were employed, and both the chemical and sensory data were auto-scaled and mean-centered. The samples were added to the model as dummy variables. Then, full cross-validation and kernel algorithm were applied.

2.9. Validation of PLS interpretations

To validate the conclusions drawn from the PLS model, we utilized the VirtuousMultiTaste platform (https://virtuous.isi.gr/#/multitaste), leveraging artificial intelligence to predict taste perceptions based on the structures of compounds. Using the simplified molecular-input line-entry system (SMILES) for compounds annotated at Level 1 ($N = 10$) and Level 2 ($N = 20$), we obtained the predicted values (%) of bitterness, sweetness, umami, and "other" for each metabolite. Then, we compared the predicted values with the interpretations of the PLS model and sought out for agreement. Furthermore, we conducted a PCA where the compounds represented scores, and the platform-predicted values represented loadings. By color-coding the scores based on the PLS interpretation, we could pinpoint the most probable compounds associated with bitterness and mouth-drying orosensation.

3. Results and discussion

3.1. Metabolome differences

To assess clustering patterns and overall sample variation of the metabolome, PCA was conducted on all detected features ($N = 41{,}151$) in faba bean samples ($N = 12$), including faba bean flour (FF), faba bean protein concentrate (FPCa, FPCb), and faba bean protein isolate (FPI). Fig. 1 displays the PCA scores (A, B) and loading plots (C, D) along the first and second components (A, C), and the first and third components (B, D). The score plot displayed clear clustering of the metabolomic profile of FPI from the other samples along the first component. In the second component, clustering of FPCb and FF underscored their common origin, whereas in the third component, clustering of FPCb and FPCa depicted the influence of dry fractionation processing rather than cultivar variation. These findings implied that both genetic variation and processing contributed to the metabolomic composition of faba bean ingredients, indicating their dual roles in shaping the biochemical composition of these fractions (Dhull et al., 2021). The loading plots suggested that FPI had a simpler metabolome than FPCa, FPCb, and FF. This implied that wet extraction of faba beans for protein isolates may result in the loss of metabolites, as previously reported for tannins, trypsin inhibitors, amino acids, raffinose family oligosaccharides, and polyols (Jeganathan et al., 2023; Vogelsang-O'Dwyer et al., 2020). Nevertheless, different extraction techniques and conditions can produce protein isolates with varying chemical compositions and functionalities, which can affect their potential in food applications (Mohan & Mellem, 2020). To the best of our knowledge, no previous study has compared the metabolomic fingerprints of commercially available faba bean fractions.

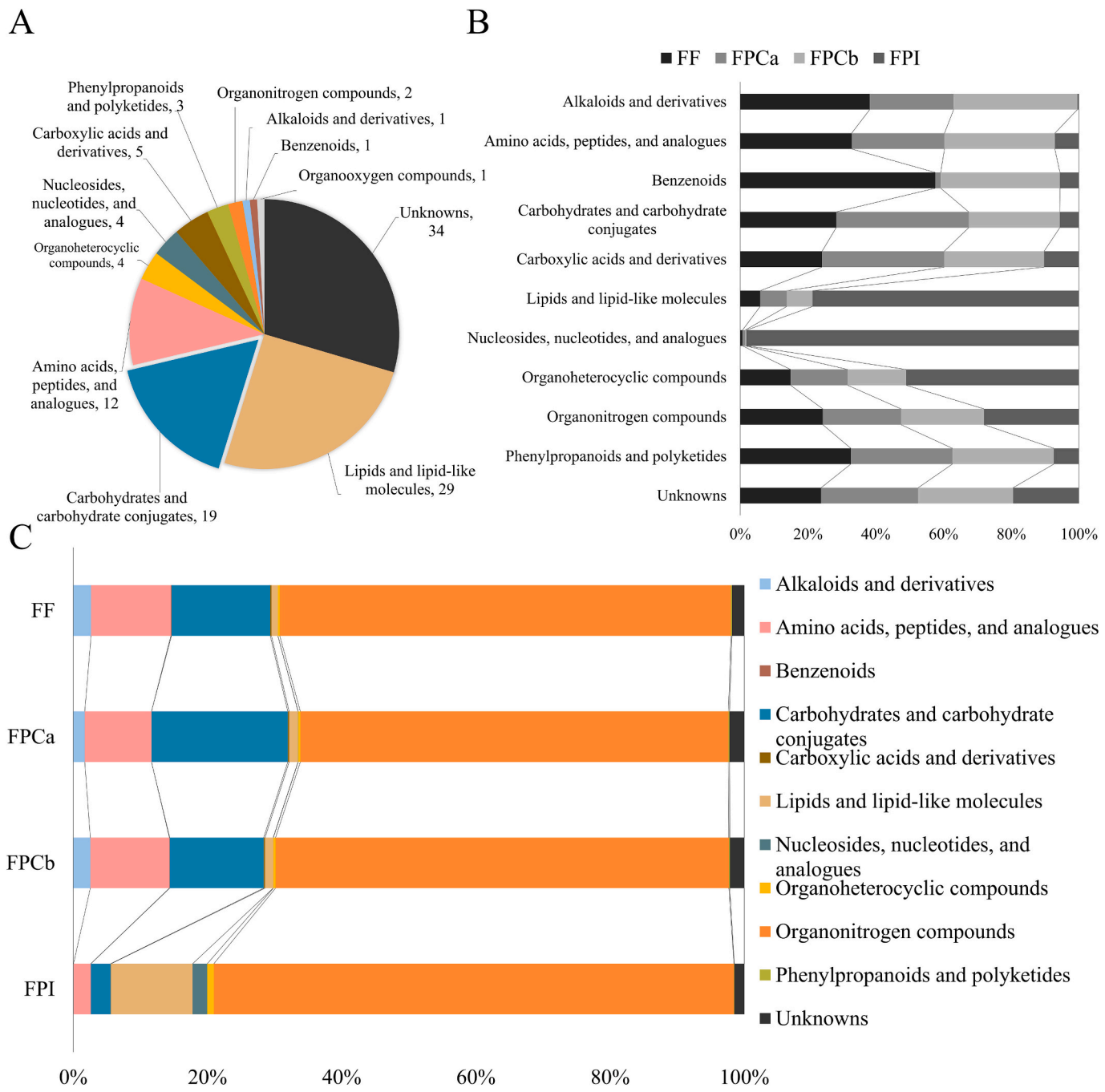

Fig. 3. Total number of annotated metabolites per compound class across all ingredients, represented as a pie chart (A). Relative abundance of the compound classes for each ingredient: faba bean flour (FF), faba bean protein concentrates (FPCa, FPCb), and faba bean protein isolate (FPI), represented as stacked bar charts (B and C).

3.2. *Differences in the abundance of annotated metabolites*

After filtering out duplicates and applying quality and relevance filters, 115 metabolites were annotated and assigned identifications at various levels (Table A1). As shown in Fig. 2, these compounds eluted between 0.8 and 11.4 min, with masses ranging between m/z 59.0136 and 997.693. The compounds with the highest peak areas were choline, vicine, betaine, trigonelline, and pipecolic acid. Choline and vicine are commonly found in many faba bean cultivars (Dhull et al., 2021; Hefni et al., 2015). While choline provides various health benefits and can be oxidized to produce betaine, which possesses essential biological roles, vicine is an antinutrient that can cause severe hemolytic anemia, known as favism, in individuals with glucose-6-phosphate dehydrogenase deficiency (Luzzatto & Arese, 2018; Zeisel & Da Costa, 2009). Trigonelline and pipecolic acid are scarcely mentioned in literature in relation to faba beans. Trigonelline is an alkaloid derived from nicotinic acid, which also has important biological functions in humans and is found in dry legume seeds as well as in sprouts (Mecha et al., 2022). Pipecolic acid is a signaling molecule derived from L-lysine metabolism that plays a role in acquired resistance in plants, and its role in faba bean likely involves stress response and defense mechanisms (Koc & Dinler, 2022).

As shown in Fig. 3, most annotated metabolites were classified as lipids, carbohydrates, and amino acids, peptides, and analogues. Fewer

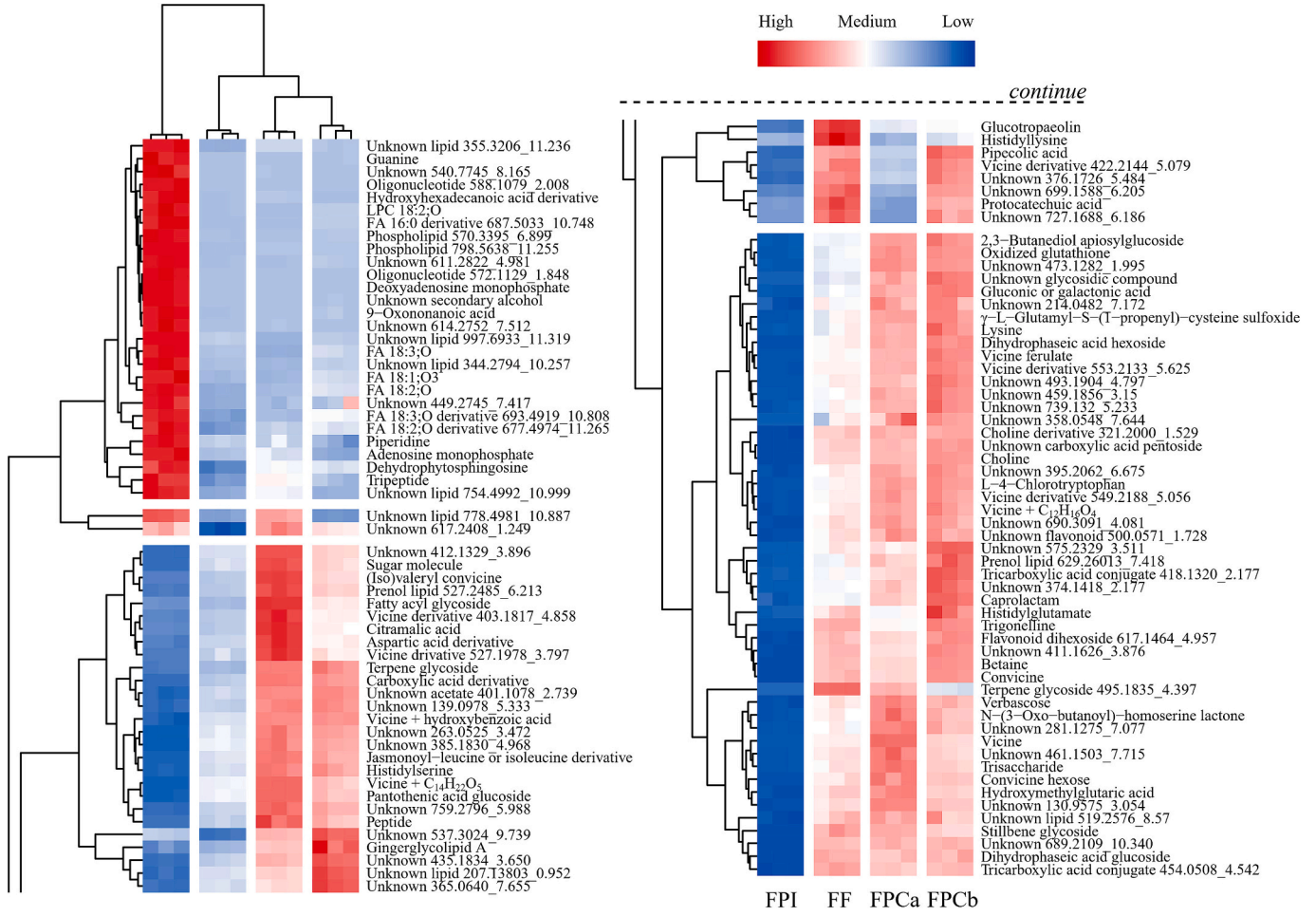

Fig. 4. Heat map of hierarchical clustering analysis based on the Euclidean distance of the relative abundance of each annotated metabolite ($N = 115$) detected in faba bean flour (FF), faba bean protein concentrates (FPCa, FPCb), and faba bean protein isolate (FPI) in three replicates ($N = 12$).

compounds belonged to organoheterocyclic-, organonitrogen-, and organooxygen- compounds; nucleosides-, nucleotides-, and analogues; carboxylic acids and derivatives; phenylpropanoids and polyketides; alkaloids and derivatives; and benzenoids. Additionally, 34 compounds could not be assigned to any specific class. Organonitrogen compounds had the highest relative abundance across all ingredients, primarily due to the high peak area of choline. FF, FPCa, and FPCb exhibited similar compound class profiles. However, FPCa showed a higher abundance of carbohydrates and a lower abundance of amino acids and peptides, compared to FF and FPCb. The relative peak area of the benzenoid protocatechuic acid was also lower in FPCa, compared to FF and FPCb. FPI had the highest abundance of nucleosides, nucleotides, lipids, and lipid-like molecules but the lowest abundance of carbohydrates, amino acids, peptides, carboxylic acids, phenylpropanoids, polyketides, and alkaloids compared to the other ingredients. This difference is likely due to the protein isolation process, which involves separating proteins from other components using wet extraction, potentially reducing the abundance of certain compound classes such as carbohydrates (Vogelsang-O'Dwyer et al., 2020). These results are specific to the filtered and annotated metabolites and do not provide insights into their proximate composition, which has been reported elsewhere (Tuccillo, Kantanen, et al., 2022).

All annotated metabolites were detected in each sample, with varying abundances across the ingredients. From HCA (Fig. 4), five clusters of compounds were identified as follows: *Cluster 1*, predominantly abundant in FPI (e.g., guanine, piperidine, dehydrophytosphingosine, along with some nucleotides, fatty acids, prenol lipids, and phospholipids); *Cluster 2*, predominantly abundant in FPI and FPCa, suggesting cultivar-specificity (two unknown compounds, of which one is a lipid); *Cluster 3*, predominantly abundant in FPCa and FPCb, potentially process-related compounds (e.g., citramalic acid and derivatives of vicine, convicine, and some amino acids); *Cluster 4*, predominantly abundant in FF and FPCb, indicating cultivar-specificity (e.g., pipecolic and protocatechuic acids); and *Cluster 5*, with the lowest abundance in FPI compared to other ingredients (e.g., vicine, convicine and their derivatives, choline and its derivative, trigonelline, betaine, caprolactam, lysine, histidylglutamate, verbascose).

Based on their fold-change (Fig. S4), we investigated the role of cultivar and processing on the abundance of annotated metabolites. The most discerning compounds in samples subjected to the same processing but of different origins were protocatechuic acid and histidyllysine (higher in FPCb, lower in FPCa), and citramalic acid (higher in FPCa, lower in FPCb). Conversely, the most discerning compounds in samples of the same origin but subjected to different processing were deoxyadenosine monophosphate (higher in FPI, lower in FPCa, and higher in FF, lower in FPCa), guanine (higher in FPI, lower in FPCa), dihydrophaseic acid hexoside (higher in FPCa, lower in FPI), histidyllysine, adenosine monophosphate, and glucotropaeolin (higher in FF, lower in FPCb), and 9-oxononanoic acid (higher in FPCb, lower in FF). Among these, protocatechuic acid was reported to be found in the seeds of cultivars Sakha and Giza, but not in their sprouts or in the variety Nubaria, supporting the hypothesis of cultivar-specificity (Mekky et al., 2020). However, little is known about the other compounds. While previous research has focused on comparative metabolite profiling

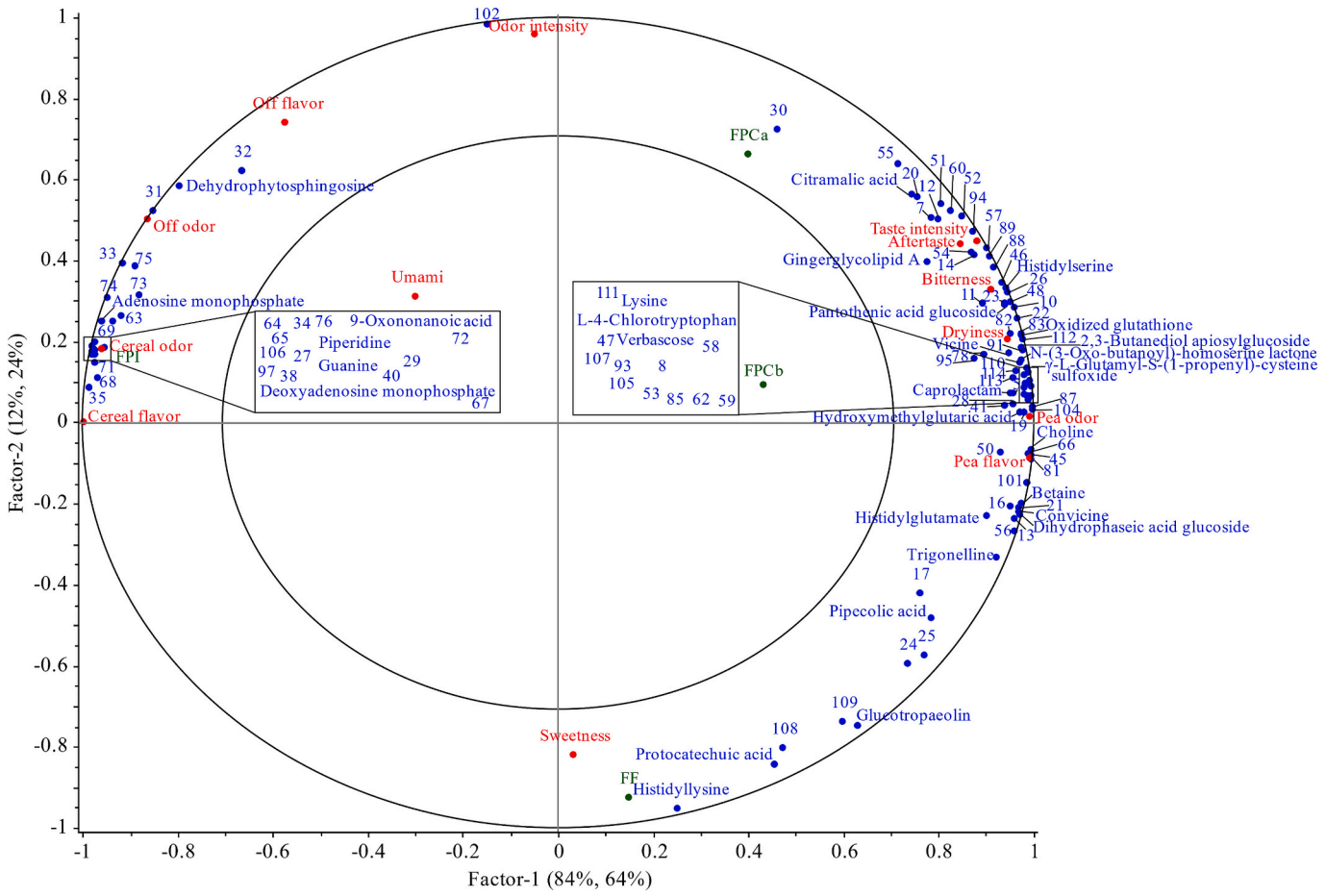

Fig. 5. Partial least squares regression (PLS) plot displaying the relationship between annotated metabolites (N = 115) (predictors, in blue) and sensory attributes (*N* = 13) (responses, in red) of faba bean flour (FF), faba bean protein concentrates (FPCa, FPCb), and faba bean protein isolate (FPI) (in green). Table A1 lists the compound names corresponding to each metabolite's ID. (For interpretation of the references to color in this figure legend, the reader is referred to the web version of this article.)

among flours of different faba bean varieties (Abu-Reidah et al., 2014; Fayek et al., 2021; Mekky et al., 2020; Valente et al., 2018, Valente et al., 2019), this is the first time that commercially available faba bean fractions have been characterized.

3.3. Metabolites associated with sensory properties

Metabolites are crucial for shaping the sensory characteristics of different food products (Wishart, 2008). However, the amount present in food does not always directly correspond to perceived intensity (Yan & Tong, 2023). Hence, even small amounts can contribute significantly to the flavor profile and induce off-flavors. To reveal the relationships between annotated metabolites and sensory properties, a regression model was applied (Fig. 5). In the PLS model, 96 % of the variation in the metabolites explained 88 % of the variation in the sensory data for the two factors. Most compounds associated with off-flavor, cereal flavor, and umami taste were various types of lipids. Phospholipids, such as Phospholipid 570.3395_6.899 and Phospholipid 798.5638_11.255, as well as the hydroxy glycerophospholipid lysophosphatidylcholine (LPC 18:2;O), can produce fatty and rancid notes through hydrolysis (Chen et al., 2023; Kumari et al., 2016). Similarly, unsaturated hydroxy fatty acids like FA 18:1;O3, FA 18:3;O, and FA 18:2;O, as well as their derivatives, can contribute to rancid off-flavors upon oxidation (Wang et al., 2022). In addition, compounds linked to umami in the PLS, such as tripeptides, oligonucleotides, and nucleotides, can interact with umami receptors and possibly heighten the receptor's response to L-glutamate (Amado et al., 2024; Morelli et al., 2022).

Only a few compounds were closely linked to sweetness, including protocatechuic acid, histidyllysine, glucotropaeolin and two unknown compounds. Conversely, several metabolites were associated with bitterness, dryness of the mouth, and strong taste and aftertaste intensities. Among these, the largest group of compounds were carbohydrates and carbohydrate conjugates, including 2,3-butanediol apiosylglucoside, verbascose, vicine, and convicine. In agreement with this study, a prior targeted analysis (Tuccillo, Kantanen, et al., 2022) found that vicine and convicine were linked to the off-flavors mentioned earlier. Furthermore, vicine and divicine derivatives were associated with bitterness in this study, although this was not investigated in the targeted analysis. While vicine is known to activate the TAS2R16 bitter taste receptor (Karolkowski, Belloir, Lucchi, et al., 2023), it has been suggested that vicine and divicine derivatives may impart bitterness also due to their β-glucopyranoside moiety (Karolkowski, Meudec, Bruguière, et al., 2023). The second largest group of compounds related to bitterness and mouth-drying orosensation were lipids of different types, including terpene and fatty acyl glycosides, prenol lipids, and fatty acids. The role of lipids and their oxidation products in modulating bitter taste has been previously reported in pea protein isolates (Gläser et al., 2021).

Furthermore, our study revealed an association between bitterness and metabolites such as lysine, histidylserine, oxidized glutathione, γ-L-glutamyl-S-(1-propenyl)-cysteine sulfoxide, as well as derivatives of aspartic acid and jasmonyl-leucine or isoleucine. The potential of small peptides to elicit a bitter taste depends on their amino acid composition and sequence, with extensive literature indicating that hydrophobic

Table 2
Predicted values (%) of bitterness, sweetness, and umami as obtained from the VirtuousMultiTaste platform for the compounds annotated at Level 1 and 2, along with the loadings of factor 1 and factor 2 in the PLS model of Fig. 5, their interpretation, and agreement with the predictions.

N	compound	factor-1	factor-2	interpretation	bitter	sweet	umami	other	agreement
1	Pipecolic acid	0.79	−0.48	Sweetness, pea flavor (*)	**40**	**51**	3	6	++
2	Vicine	0.95	0.17	Bitterness, dryness, taste intensity, aftertaste	**27**	**27**	**28**	17	+
3	Deoxyadenosine monophosphate	−0.98	0.17	Umami, cereal flavor, off-flavor	2	2	**95**	1	++
4	Guanine	−0.98	0.17	Umami, cereal flavor, off-flavor	**35**	**35**	4	**26**	–
6	Caprolactam	0.95	0.07	Bitterness, dryness, taste intensity, aftertaste	**47**	19	**27**	6	++
9	γ-L-Glutamyl-S-(1-propenyl)-cysteine sulfoxide	0.99	0.13	Bitterness, dryness, taste intensity, aftertaste	16	22	**40**	22	–
15	L-4-Chlorotryptophan	0.99	0.10	Bitterness, dryness, taste intensity, aftertaste	**34**	**41**	7	18	+
18	Glucotropaeolin	0.63	−0.75	Sweetness, pea flavor (*)	**45**	17	6	**32**	+
36	Oxidized glutathione	0.97	0.21	Bitterness, dryness, taste intensity, aftertaste	7	3	**79**	11	–
37	Citramalic acid	0.74	0.56	Bitterness, dryness, taste intensity, aftertaste	7	23	**38**	**32**	–
39	Protocatechuic acid	0.45	−0.84	Sweetness, pea flavor	**31**	**42**	22	5	++
42	N-(3-Oxo-butanoyl)-homoserine lactone	0.98	0.16	Bitterness, dryness, taste intensity, aftertaste	**38**	**53**	3	6	+
43	2,3-Butanediol apiosylglucoside	0.98	0.19	Bitterness, dryness, taste intensity, aftertaste	16	**33**	12	**39**	–
44	Pantothenic acid glucoside	0.94	0.29	Bitterness, dryness, taste intensity, aftertaste	**25**	15	**47**	13	+
49	Dihydrophaseic acid glucoside	0.97	−0.23	Sweetness, pea flavor (*)	**47**	24	5	23	+
61	9-Oxononanoic acid	−0.98	0.18	Umami, cereal flavor, off-flavor	**39**	**38**	3	20	–
70	Gingerglycolipid A	0.78	0.40	Bitterness, dryness, taste intensity, aftertaste	**46**	**28**	8	18	++
77	Dehydrophytosphingosine	−0.80	0.58	Umami, cereal flavor, off-flavor	**62**	13	6	14	–
79	Piperidine	−0.98	0.18	Umami, cereal flavor, off-flavor	**80**	18	0	2	–
80	Choline	1.00	−0.07	Sweetness, pea flavor (*)	**31**	**50**	3	16	++
84	Betaine	0.97	−0.20	Sweetness, pea flavor (*)	**54**	**28**	4	14	++
86	Trigonelline	0.92	−0.33	Sweetness, pea flavor (*)	**37**	**57**	2	4	++
90	Convicine	0.97	−0.22	Sweetness, pea flavor (*)	23	**28**	**33**	16	+
92	Adenosine monophosphate	−0.96	0.25	Umami, cereal flavor, off-flavor	0	0	**100**	0	++
96	Lysine	0.98	0.12	Bitterness, dryness, taste intensity, aftertaste	**36**	**35**	20	9	++
98	Histidylglutamate	0.90	−0.23	Sweetness, pea flavor (*)	1	0	**96**	3	–
99	Histidylserine	0.94	0.33	Bitterness, dryness, taste intensity, aftertaste	18	**32**	**37**	14	–
100	Hydroxymethylglutaric acid	0.97	0.03	Bitterness, dryness, taste intensity, aftertaste	16	**26**	**38**	20	–
103	Histidyllysine	0.25	−0.95	Sweetness, pea flavor	**43**	19	**36**	2	–
115	Verbascose	0.99	0.10	Bitterness, dryness, taste intensity, aftertaste	8	**74**	9	8	–

* Indicates that the interpretation could also include bitterness, dryness, taste intensity, and aftertaste. Values in bold are above the average. Agreement levels: "-" disagreement, "+" moderate agreement, and "++" strong agreement.

amino acids (e.g., leucine and isoleucine) can lead to bitterness (Wang et al., 2023). Moreover, lysine, which was also linked to bitterness in the targeted analysis (Tuccillo, Kantanen, et al., 2022) and previously described as a bitter amino acid (Sonntag et al., 2010), was also found to suppress the bitterness of quinine (Zhang et al., 2016). Finally, organoheterocyclic caprolactam and L-4-chlorotryptophan were also associated with bitterness. Notably, caprolactam is known to activate the bitter taste receptor hTAS2R38 (Meyerhof et al., 2010).

Overall, the flavor of faba bean ingredients can be influenced by a variety of factors, and while some compounds may contribute to bitterness and mouth-drying orosensation, others might suppress it or interact with taste receptors, other compounds, and the matrix in several ways (Karolkowski, Belloir, Briand, & Salles, 2023; Tuccillo, Kantanen, et al., 2022; Wang et al., 2022, 2024).

3.4. Model-platform consistency assessment

We validated the conclusions from the PLS model against the VirtuousMultiTaste platform for compounds annotated at Level 1 and Level 2 and characterized by a SMILES, whose structures are shown in Fig. S5. Table 2 shows that among the compounds associated with the umami taste in the PLS model, only adenosine and deoxyadenosine monophosphates were confirmed by the platform as umami ligands. Similarly, protocatechuic acid was the only compound mainly associated with a sweet taste by both the PLS model and the platform. However, when tested in water at a concentration of 2 g/L, protocatechuic acid showed moderate astringency and slight bitterness (Ferrer-Gallego et al., 2014). Moreover, the persistence and intensity of astringency increased when protocatechuic acid was tasted in the presence of unpleasant aromas (Ferrer-Gallego et al., 2014). This discrepancy aligns with the findings from the PLS plot, where compounds located in the same PLS plot quadrant as sweetness could also be interpreted as associated with bitterness, dryness, taste intensity, and aftertaste, as they were positively located on Factor 1. Among these, pipecolic acid, choline, betaine, and trigonelline were predicted by the platform as both sweet and bitter, while convicine was predicted as sweet and umami. Additionally, glucotropaeolin and dihydrophaseic acid glucoside were predicted as bitter.

Regarding compounds associated with bitterness, mouth dryness, and strong taste and aftertaste intensities in the PLS model, the platform confirmed these associations for caprolactam, gingerglycolipid A, lysine, vicine, L-4-chlorotryptophan, N-(3-oxo-butanoyl)-homoserine lactone, and pantothenic acid glucoside. Conversely, the platform did not predict the following compounds as bitter, indicating that associations from the PLS model regarding their bitterness should be interpreted with caution: γ-L-glutamyl-S-(1-propenyl)-cysteine sulfoxide, oxidized glutathione, citramalic acid, 2,3-butanediol apiosylglucoside, histidylserine, hydroxymethylglutaric acid, and verbascose.

This facilitated the identification of any disparities or agreements between the model's predictions and platform perceptions. However, these conclusions were limited to using only one machine learning tool that considers only the chemical structure and not interaction and suppression effects. A recently developed tool to predict the bitter taste of molecules, BitterMasS, may enable the identification of bitter compounds based on spectrum-based predictions (Ziaikin et al., 2023). Although many predictive tools have been developed to evaluate the bitterness of suspected bitterants, they cannot provide unequivocal identification of new bitter compounds, as isolation and purification procedures are still necessary (Yan & Tong, 2023). Despite its limitations, the platform combined with sensory data of the samples may be used to prioritize and narrow down candidate compounds linked to the taste of interest, helping to streamline interventions such as genetic improvement and targeted processing.

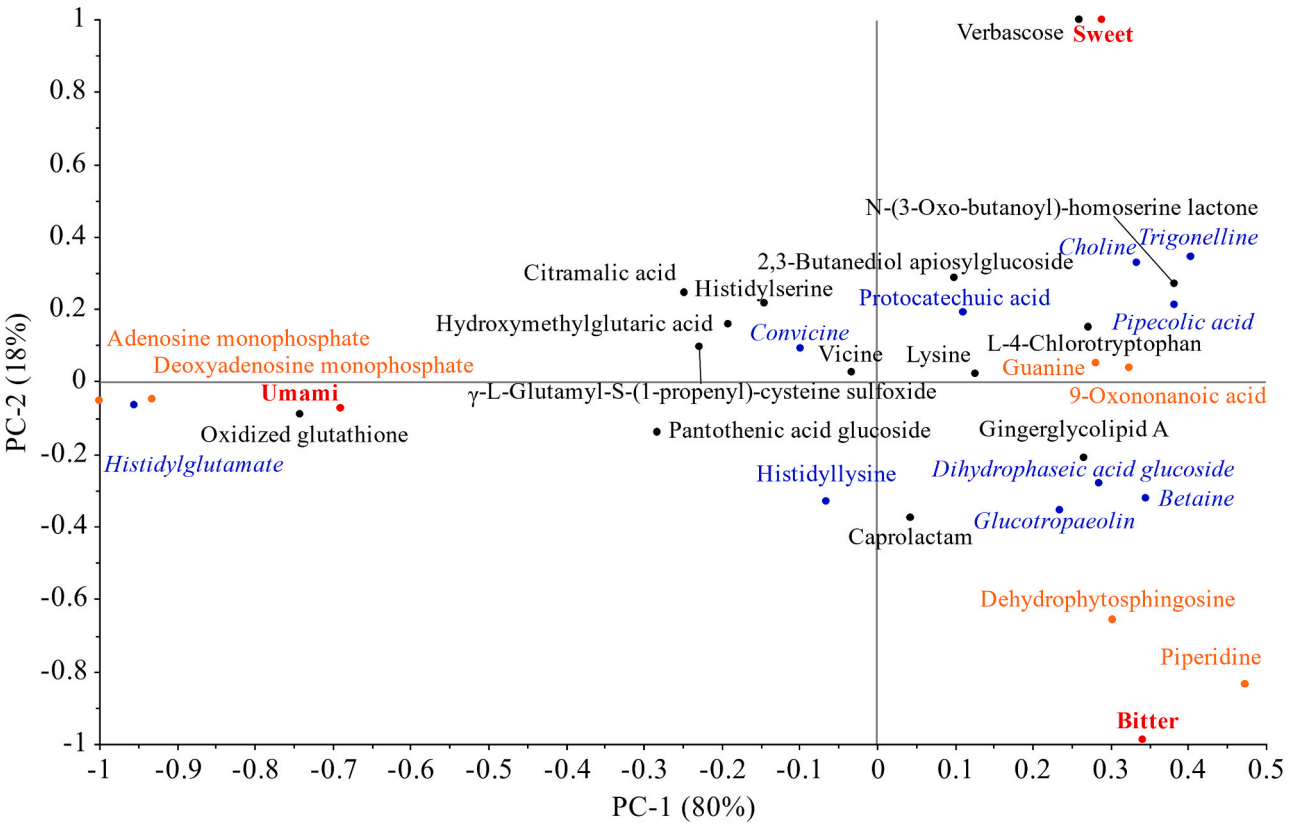

Fig. 6. Principal Component Analysis (PCA) bi-plot illustrating the annotated metabolites at Level 1 ($N = 10$) and Level 2 ($N = 20$), and their predicted values (%) of bitterness, sweetness, and umami from the VirtuousMultiTaste platform. Scores were color-coded based on their association with the loadings of the PLS model (see Fig. 6) as follows: in black, compounds associated with bitterness, dryness, taste intensity, and aftertaste; in blue, compounds associated with sweetness and pea flavor (in italics could also be associated with bitterness, dryness, taste intensity, and aftertaste); in orange, compounds associated with umami, cereal flavor, and off-flavor. (For interpretation of the references to color in this figure legend, the reader is referred to the web version of this article.)

Furthermore, PCA helped understand the overall structure of the data and assess the relationship between metabolites and predicted tastes on the platform by reducing dimensionality. Fig. 6 illustrates the compounds that displayed consistency between PLS and platform predictions, thereby further strengthening the validity of our conclusions regarding potential metabolites associated with off-flavors in faba bean ingredients. A list of potential compounds linked to bitterness, mouth-drying orosensation, and high taste and aftertaste intensities in the faba bean ingredients of this study included caprolactam, gingerglycolipid, lysine, vicine, L-4-chlorotryptophan, and potentially glucotropaeolin, betaine, dihydrophaseic acid glucoside, convicine, and pipecolic acid. Among these compounds, only lysine was present in the BitterBD database of bitter taste ligands (Dagan-Wiener et al., 2019), indicating the novelty of most of the compounds associated with off-flavors of faba bean ingredients in our research.

3.5. Limitations

Although this study highlighted variations in the abundance of potential non-volatile sensory-relevant metabolites among the ingredients, our specific filtering criteria limited the exploration of the full metabolomic differences across cultivars and processing methods. These criteria were necessary due to the large dataset and the presence of low-quality features, which made it impractical to examine the entire metabolomic profile. This is a common limitation in large-scale studies rather than a shortcoming of the protocol itself (Klåvus et al., 2020). Additionally, our extraction method may have led to the loss or omission of metabolites significant to flavor.

To fully understand the sensory properties of foods, both volatile and non-volatile compounds are important (Wang et al., 2022). The current study focused on potential non-volatile flavor-active compounds, which were utilized as predictive variables in a model that also included odor-related responses (e.g., pea odor, off-odor). We chose not to remove them to evaluate the relationship across the entire sensory profile. The relationship between potential volatile flavor-active compounds and odor-related attributes in these samples has been reported elsewhere (Tuccillo, Kantanen, et al., 2022).

While our method employs descriptive sensory analysis, alternative approaches, such as dose-over-threshold factor analysis and taste dilution analysis, should be considered for establishing causality and dose-dependent contribution to taste. Nonetheless, this study examines the non-volatile metabolites of faba bean ingredients within their complex food matrix. Tasting of isolated individual compounds may not accurately represent their sensory contributions in faba bean-based foods, and similar approaches to this study have been applied to other foods.

Finally, in discussing genetic variability and cultivar-related differences, external factors such as soil, climate, and agricultural practices, which also influence genetic variability and flavor, were not considered in this study. As commercially available faba bean ingredients were used, such information is unavailable in the current dataset.

4. Conclusions

Our study revealed that variations in the metabolome of faba bean ingredients were influenced by both processing methods and genetic variability. Regression modeling identified specific metabolites associated with sensory attributes, such as bitterness and mouth-drying sensation, shedding light on the potential contributors to off-flavors, including caprolactam, gingerglycolipid, lysine, vicine, and convicine among others. Validation against a predictive platform underscored the

consistency of certain metabolite associations with sensory perceptions, thereby providing valuable insights for targeted flavor optimization strategies.

Furthermore, these findings highlight the potential of metabolomics-based approaches for elucidating the flavor chemistry underlying minimally processed plant-based protein ingredients. The list of potential bitter-causing compounds in faba bean ingredients could be a foundation for further studies on the bitterness of these compounds in their isolated and purified forms, as well as investigations at the receptor level. Despite significant efforts, there is a severe lack of information regarding varied bitter compounds found in food, henceforth, many issues remain unresolved (Yan & Tong, 2023).

CRediT authorship contribution statement

Fabio Tuccillo: Writing – review & editing, Writing – original draft, Visualization, Methodology, Investigation, Formal analysis, Data curation, Conceptualization. **Anna Kårlund:** Writing – review & editing, Methodology, Investigation, Formal analysis, Data curation, Conceptualization. **Ville Koistinen:** Writing – review & editing, Methodology, Data curation. **Shania Saini:** Writing – review & editing, Data curation. **Hany Ahmed:** Writing – review & editing, Formal analysis, Conceptualization. **Kati Hanhineva:** Writing – review & editing, Supervision, Resources, Conceptualization. **Mari Sandell:** Writing – review & editing, Supervision, Conceptualization. **Kati Katina:** Writing – review & editing, Supervision, Funding acquisition, Conceptualization. **Anna-Maija Lampi:** Writing – review & editing, Supervision, Conceptualization.

Declaration of competing interest

The authors declare that they have no known competing financial interests or personal relationships that could have appeared to influence the work reported in this paper.

Acknowledgements

The authors acknowledge financial support from The University of Helsinki Doctoral School (UHDS) and the project HealthFerm, which is co-funded by the European Union under the Horizon Europe grant agreement No. 101060247 and the Swiss State Secretariat for Education, Research and Innovation (SERI) under contract No. 22.00210. Views and opinions expressed are however those of the author(s) only and do not necessarily reflect those of the European Union or European Research Executive Agency (REA). Neither the European Union nor REA can be held responsible for them.

Appendix A. Appendices

Table A1
Potential sensory-relevant annotated metabolites.

	ion mode	RT (min)	M_{obs}	M_{mi}	adduct	formula	annotation	*m/z* (intensity)*	compound classification	ID	ref
1	RP+	0.779	130.0863	129.0785	[M + H]+	$C_6H_{11}NO_2$	Pipecolic acid	84.0808 (100), 56.04887 (6)	Amino acids, peptides, and analogues	1	A, B, C
2	RP+	0.853	305.1109	304.1031	[M + H]+	$C_{10}H_{16}N_4O_7$	Vicine	143.0571 (100)	Carbohydrates and carbohydrate conjugates	1	A, B, C
3	RP+	1.036	332.0752	331.0673	[M + H]+	$C_{10}H_{14}N_5O_6P$	Deoxyadenosine monophosphate	136.0615 (100), 81.0331 (21), 314.1252 (5)	Nucleosides, nucleotides, and analogues	1	A, B, C
4	RP+	1.994	152.0567	151.0489	[M + H]+	$C_5H_5N_5O$	Guanine	110.0342 (100), 152.0564 (99), 135.0305 (52)	Organoheterocyclic compounds	2	A, B
5	RP+	2.177	374.1418	373.1339	[M + H]+	n/a	Unknown 374.1418_2.177	374.1472 (100), 330.1507 (36)	n/a	4	n/a
6	RP+	2.846	114.0913	113.0835	[M + H]+	$C_6H_{11}NO$	Caprolactam	114.09072 (100), 55.0527 (6)	Organoheterocyclic compounds	2	B
7	RP+	3.001	133.0376	217.0922	[M-84.06 + H]+	n/a	Aspartic acid derivative	134.0449 (100), 88.0394 (22), 116.0355 (11), 74.0231 (8) (218.0995 (8; [M + H]+)	Amino acids, peptides, and analogues	3	M
8	RP+	3.267	927.3525	444.1986	[2 M + K]	$C_{21}H_{32}O_{10}$	Dihydrophaseic acid hexoside	483.1534 (100; [M + K]+), 303.0947 (7; [aglyc. + K]+), 927.3475 (3; [2 M + K]+), aglycone: 247.1324 (100;[M + H]+), 175.0751 (85), 265.1432 (84), 203.1063 (77)	Lipids and lipid-like molecules	3	J, N
9	RP+	3.390	307.0923	306.0845	[M + H]+	$C_{11}H_{18}N_2O_6S$	γ-L-Glutamyl-S-(1-propenyl)-cysteine sulfoxide	261.0871 (100), 130.0649 (48), 289.0825 (36), 307.0926 (27), 243.0721 (11)	Amino acids, peptides, and analogues	2	B
10	RP+	3.472	263.0525	240.0633	[M + Na]+	n/a	Unknown 263.0525_3.472	263.0529 (100), 143.0327 (92),	n/a	4	n/a

(*continued on next page*)

Table A1 (*continued*)

	ion mode	RT (min)	M_{obs}	M_{mi}	adduct	formula	annotation	*m/z* (intensity)*	compound classification	ID	ref
								120.0814 (53), 208.1073 (28)			
11	RP+	3.650	435.1834	434.1756	[M + H]+	n/a	Unknown 435.1834_3.650	435.1846 (100), 303.1403 (86), 237.0568 (50), 216.9771 (84)	n/a	4	n/a
12	RP+	3.797	527.1978	526.1900	[M + H]+	n/a	Vicine derivative 527.1978_3.797	527.1966 (100), 143.0565 (8)	Carbohydrates and carbohydrate conjugates	3	K
13	RP+	3.876	411.1626	388.1734	[M + Na]+	n/a	Unknown 411.1626_3.876	165.0151 (100), 179.0333 (28), 86.0969 (23), 103.0745 (5), 119.0503 (1) (411.1639; [M + Na]+)	n/a	4	n/a
14	RP+	3.896	412.1329	389.1437	[M + Na]+	n/a	Unknown 412.1329_3.896	144.0406 (100), 390.1500 (30; [M + H]+), 229.1076 (17), 85.0650 (16) (412.1327; [M + Na]+)	n/a	4	n/a
15	RP+	3.998	239.0581	238.0503	[M + H]+	$C_{11}H_{11}ClN_2O_2$	L-4-Chlorotryptophan	222.0316 (100), 180.0219 (44), 239.0583 (32), 193.0542 (18), 166.0430 (6), 204.0220 (2)	Organoheterocyclic compounds	2	C
16	RP+	4.310	421.1466	420.1388	[M + H]+	n/a	Stilbene glycoside	243.0391 (100), 147.0462 (3)	Phenylpropanoids and polyketides	3	C
17	RP+	4.397	495.1835	472.1943	[M + Na]+	n/a	Terpene glycoside 495.1835_4.397	120.0801 (100), 247.1303 (69), 409.1830 (47)	Lipids and lipid-like molecules	3	J
18	RP+	4.774	410.0612	409.0534	[M + H]+	C14H19NO9S2	Glucotropaeolin	410.0631 (100), 248.0078 (47)	Carbohydrates and carbohydrate conjugates	2	C
19	RP+	4.797	493.1904	470.2012	[M + Na]+	n/a	Unknown 493.1904_4.797	164.0309 (100), 493.1856 (10)	n/a	4	n/a
20	RP+	4.858	403.1817	402.1738	[M + H]+	n/a	Vicine derivative 403.1817_4.858	143.0566 (100), 367.1655 (18), 305.1111 (7)	Carbohydrates and carbohydrate conjugates	3	K
21	RP+	4.957	617.1464	594.1571	[M + Na]+	n/a	Flavonoid dihexoside 617.1464_4.957	287.0536 (100), 85.0277 (24); (617.1473; [M + Na]+)	Phenylpropanoids and polyketides	3	B, C
22	RP+	4.968	385.1830	384.1752	[M + H]+	n/a	Unknown 385.1830_4.968	265.1426 (100), 256.1061 (62), 69.0691 (57), 161.0651 (51), 385.1833 (22), 149.0973 (18)	n/a	4	n/a
23	RP+	5.067	575.2554	574.2475	[M + H]+	$C_{24}H_{38}N_4O_{12}$	Vicine + $C_{14}H_{22}O_5$	575.2559 (100), 143.0566 (40)	Carbohydrates and carbohydrate conjugates	3	K
24	RP+	5.079	422.2144	399.2252	[M + Na]+	n/a	Vicine derivative 422.2144_5.079	422.2143 (100), 143.0566 (22)(, 400.2336 [M + H]+)	Carbohydrates and carbohydrate conjugates	3	K
25	RP+	5.484	376.1726	353.1834	[M + Na]+	n/a	Unknown 376.1726_5.484	376.1731 (100), 147.0793 (34), 184.1344 (23), 230.1201 (7)	n/a	4	n/a
26	RP+	6.084	568.2726	567.2647	[M + H]+	n/a	Jasmonoyl-leucine or isoleucine derivative	324.2162 (100), 486.2687 (65), 384.2381 (39), 193.1210 (28), 546.2907 (20), 132.1005 (1)	Amino acids, peptides, and analogues	3	J
27	RP+	6.899	570.3395	569.3317	[M + H]+	n/a	Phospholipid 570.3395_6.899	pos: 570.3417 (100), 184.0736 (57), 552.3315 (23), 104.1066 (18); neg: 554.3070 (100), 329.2376 (12), 483.2331 (11)	Lipids and lipid-like molecules	3	G

(*continued on next page*)

Table A1 (*continued*)

	ion mode	RT (min)	M_{obs}	M_{mi}	adduct	formula	annotation	*m/z* (intensity)*	compound classification	ID	ref
28	RP+	7.418	629.2601	628.2523	[M + H]+	n/a	Prenol lipid 629.26013_7.418	585.2709 (100), 299.1396 (52), 611.2461 (41), 629.2605 (41)	Lipids and lipid-like molecules	3	L
29	RP+	8.224	421.1629	420.1550	[M + H]+	n/a	Unknown secondary alcohol	399.1824 (100), 301.2127 (84), 319.2260 (71), 235.1298 (18), 195.0997 (14)	Organooxygen compounds	3	C
30	RP+	9.739	537.3024	536.2945	[M + H]+	n/a	Unknown 537.3024_9.739	537.3017 (100)	n/a	4	n/a
31	RP+	10.674	976.5717	488.2859	[2 M + H]+	$C_{23}H_{36}N_8O_4$	Tripeptide	977.5782 (100)	Amino acids, peptides, and analogues	3	N
32	RP+	10.887	778.4981	777.4902	[M + H]+	n/a	Unknown lipid 778.4981_10.887	778.4985 (100), 760.4890 (25), 590.4836 (11)	Lipids and lipid-like molecules	4	B, D
33	RP+	10.999	754.4992	753.4914	[M + H]+	n/a	Unknown lipid 754.4992_10.999	754.4950 (100), 736.4911 (74)	Lipids and lipid-like molecules	4	B, D
34	RP+	11.255	798.5638	797.5559	[M + H]+	n/a	Phospholipid 798.5638_11.255	pos: 798.5637 (100), 184.0750 (11), 104.1063 (1); neg: 281.2456 (100), 279.2320 (79), 295.2276 (43), 782.5369 (26)	Lipids and lipid-like molecules	3	G
35	RP+	11.319	997.6933	955.6595	[M + ACN + H]+	n/a	Unknown lipid 997.6933_11.319	997.6913 (100), 282.2793 (8)	Lipids and lipid-like molecules	4	D
36	RP-	1.201	611.1427	612.1505	[M-H]-	$C_{20}H_{32}N_6O_{12}S_2$	Oxidized glutathione	611.1414 (100), 306.0729 (22), 272.0859 (18), 128.0362 (10), 254.0773 (9)	Amino acids, peptides, and analogues	2	G
37	RP-	1.236	147.0294	148.0373	[M-H]-	$C_5H_8O_5$	Citramalic acid	87.0082 (100), 147.0282 (51), 85.02946 (29), 129.0208 (10)	Carboxylic acids and derivatives	1	A, B, E
38	RP-	1.848	572.1129	573.1208	[M-H]-	n/a	Oligonucleotide 572.1129_1.848	572.1129 (100), 111.0200 (85), 460.0840 (24), 346.0538 (21), 78.9586 (9)	Nucleosides, nucleotides, and analogues	3	C
39	RP-	1.910	153.0190	154.0268	[M-H]-	$C_7H_6O_4$	Protocatechuic acid	153.0188 (100), 135.0083 (19), 107.0124 (16)	Benzenoids	2	A, B, E
40	RP-	2.008	588.1079	589.1158	[M-H]-	n/a	Oligonucleotide 588.1079_2.008	588.1097 (100), 78.9593 (23), 150.0436 (20), 362.0503 (17)	Nucleosides, nucleotides, and analogues	3	C
41	RP-	2.177	418.1320	351.1536	[M + 67.99-H]-	n/a	Tricarboxylic acid conjugate 418.1320_2.177	306.1559 (100), 350.1463 (50; [M-H]-), 144.1010 (43); (418.1327; [M + 67.99-H]-)	Carboxylic acids and derivatives	3	C
42	RP-	2.359	184.0615	185.0690	[M-H]-	$C_8H_{11}NO_4$	N-(3-Oxo-butanoyl)-homoserine lactone	184.0616 (100), 59.0149 (18), 140.0693 (14)	Lipids and lipid-like molecules	2	A, D
43	RP-	2.450	383.1548	384.1626	[M-H]-	$C_{15}H_{28}O_{11}$	2,3-Butanediol apiosylglucoside	101.0244 (100), 251.1137 (48), 383.2072 (47), 99.0079 (35), 71.0139 (33)	Carbohydrates and carbohydrate conjugates	2	B, F
44	RP-	2.519	448.1418	381.1627	[M + 67.99-H]-	$C_{15}H_{27}NO_{10}$	Pantothenic acid glucoside	146.0821 (100), 380.1532 (91), 71.0135 (36), 308.1335 (32), 89.0247 (15)	Fatty acyl glycosides	2	C, J
45	RP-	2.681	259.1180	260.1258	[M-H]-	$C_{12}H_{20}O_6$	Unknown carboxylic acid pentoside	127.0763 (100), 259.1181 (64), 109.0659 (49)	Carboxylic acids and derivatives	3	O
46	RP-	2.739	401.1078	402.1157	[M-H]-	n/a	Unknown acetate 401.1078_2.739	401.1060 (100), 341.0855 (95), 177.0545 (68),	n/a	4	n/a

(*continued on next page*)

Table A1 (*continued*)

	ion mode	RT (min)	M_{obs}	M_{mi}	adduct	formula	annotation	*m/z* (intensity)*	compound classification	ID	ref
								149.0605 (55), 195.0667 (29)			
47	RP-	3.150	459.1856	460.1935	[M-H]-	n/a	Unknown 459.1856_3.15	459.1910 (100), 71.0141 (34), 73.0323 (31), 89.0235 (27)	n/a	4	n/a
48	RP-	3.223	423.112	424.1225	[M-H]-	$C_{17}H_{20}N_4O_9$	Vicine + hydroxybenzoic acid	141.0412 (100), 423.1158 (74), 303.0943 (17)	Carbohydrates and carbohydrate conjugates	3	K
49	RP-	3.281	579.1655	444.1996	[M + 135.97-H]-	$C_{21}H_{32}O_{10}$	Dihydrophaseic acid glucoside	443.1903 (100; [M-H]-), 237.1481 (5), 161.0462 (5), 219.1363 (4), 281.1357 (4); (579.1606; [M + 135.97-H]-)	Lipids and lipid-like molecules	2	D, J
50	RP-	3.511	575.2329	576.2407	[M-H]-	n/a	Unknown 575.2329_3.511	247.0790 (100)	n/a	4	n/a
51	RP-	3.894	502.1281	389.1426	[M + 112.99-H]-	$C_{15}H_{23}N_3O_9$	(Iso)valeryl convicine	388.1353 (100), 502.1273 (6; [M + 112.99-H]-), 141.0167 (2)	Carbohydrates and carbohydrate conjugates	3	K
52	RP-	4.143	631.2202	518.2381	[M + 112.99-H]-	n/a	Terpene glycoside	517.2308 (100; [M-H]-), 99.0084 (75), 385.1877 (54), 101.0253 (36), 223.1346 (19); (631.2200; [M + 112.99-H]-)	Lipids and lipid-like molecules	3	C
53	RP-	4.197	479.1406	480.1484	[M-H]-	$C_{20}H_{24}N_4O_{10}$	Vicine ferulate	337.0904 (100), 479.1427 (70), 141.0423 (68), 193.0472 (22), 175.0394 (22), 303.0914 (16)	Carbohydrates and carbohydrate conjugates	3	K
54	RP-	4.266	59.0136	60.0214	[M-144.08-H]-	n/a	Sugar	59.0137 (100); (99.0817 (25), 143.0731 (8), 203.0928 ([M-H]-))	Carbohydrates and carbohydrate conjugates	3	L
55	RP-	4.275	519.2432	520.2511	[M-H]-	$C_{24}H_{40}O_{12}$	Fatty acyl glycoside	519.2404 (100), 387.2010 (35), 225.1497 (28), 101.0254 (25)	Lipids and lipid-like molecules	3	B, C
56	RP-	4.542	454.0508	387.0721	[M + 67.99-H]-	n/a	Tricarboxylic acid conjugate 454.0508_4.542	224.0109 (100), 180.0215 (68), 386.0648 (57; [M-H]-); (454.0522; [M + 67.99-H]-)	Carboxylic acids and derivatives	3	C
57	RP-	4.687	307.1389	308.1467	[M-H]-	n/a	Carboxylic acid derivative	145.0862 (100), 71.0133 (25), 280.0493 (18), 73.029 (13), 307.1397 (12), 127.0783 (8), 89.0236 (8)	Carboxylic acids and derivatives	3	C
58	RP-	5.056	549.2188	550.2266	[M-H]-	n/a	Vicine derivative 549.2188_5.056	549.2202 (100), 141.0410 (80), 303.0903 (55)	Carbohydrates and carbohydrate conjugates	3	K
59	RP-	5.625	553.2133	554.2212	[M-H]-	n/a	Vicine derivative 553.2133_5.625	553.2119 (100), 303.0941 (28), 141.0419 (25)	Carbohydrates and carbohydrate conjugates	3	K
60	RP-	6.213	527.2485	560.2817	[M-CH4O-H]-	n/a	Prenol lipid 527.2485_6.213	559.2744 (100; [M-H]-), 179.0555 (81), 89.0250 (53), 351.2163 (35), 119.0348 (20)	Lipids and lipid-like molecules	3	P, Q
61	RP-	6.353	171.1023	172.1102	[M-H]-	$C_9H_{16}O_3$	9-Oxononanoic acid	127.1115 (100), 153.0904 (44), 171.1014 (24), 57.03398 (19)	Lipids and lipid-like molecules	2	B, D, E
62	RP-	6.675	395.2062	396.2141	[M-H]-	n/a	Unknown 395.2062_6.675	190.930 (100), 307.3945 (98), 243.4557 (79), 75.5204 (70), 261.1872 (68)	n/a	4	n/a

(*continued on next page*)

Table A1 (*continued*)

	ion mode	RT (min)	M_{obs}	M_{mi}	adduct	formula	annotation	*m/z* (intensity)*	compound classification	ID	ref
63	RP-	7.417	449.2745	450.2823	[M-H]-	n/a	Unknown 449.2745_7.417	329.2337 (100)	n/a	4	n/a
64	RP-	7.512	614.2752	615.2830	[M-H]-	n/a	Unknown 614.2752_7.512	79.9561 (100), 295.2273 (80), 239.3931 (73), 63.1546 (69), 253.9766 (65)	n/a	4	n/a
65	RP-	7.652	465.2068	330.2403	[M + 135.97-H]-	$C_{18}H_{34}O_5$	FA 18:1;O3	329.2330 (100; [M-H]-), 211.1330 (95), 229.1426 (59), 171.1023 (54), 99.0818 (19), 311.2184 (18); (465.2125; [M + 135.97-H]-)	Lipids and lipid-like molecules	3	C, D
66	RP-	8.570	519.2576	520.2655	[M-H]-	n/a	Unknown lipid 519.2576_8.57	315.1961 (100)	Lipids and lipid-like molecules	4	D
67	RP-	8.779	648.3112	535.3264	[M + 112.99-H]-	n/a	LPC 18:2;O	neg: 520.3019 (100), 295.2257 (34), 224.0688 (13), 580.3211 (6; [M + FA-H]-), pos: 518.3228 (100), 184.0728 (94), 104.1066 (57)	Lipids and lipid-like molecules	3	D
68	RP-	9.151	429.1854	294.2197	[M + 135.97-H]-	C18H30O3	FA 18:3;O	275.1997 (100), 293.2109 (84; [M-H]-), 171.1014 (32), 121.1032 (20); (429.1877; [M + 135.97-H]-)	Lipids and lipid-like molecules	3	C
69	RP-	9.413	431.2011	296.2351	[M + 135.97-H]-	C18H32O3	FA 18:2;O	295.2271 (100; [M-H]-), 277.2177 (14), 195.1375 (12); (431.2031; [M + 135.97-H]-)	Lipids and lipid-like molecules	3	C
70	RP-	9.508	721.3629	676.3646	[M + FA-H]-	$C_{33}H_{56}O_{14}$	Gingerglycolipid A	675.3564 (100; [M-H]-), 397.1373 (26), 721.3609 (15), 277.2186 (15), 415.1453 (5)	Lipids and lipid-like molecules	2	B, C, D
71	RP-	10.257	344.2794	299.2812	[M + FA-H]-	n/a	Unknown lipid 344.2794_10.257	248.9601 (100), 94.9616 (39), 205.1207 (38), 209.1939 (31), 301.2472 (30)	Lipids and lipid-like molecules	4	B, D
72	RP-	10.748	687.5033	642.5069	[M + FA-H]-	n/a	FA 16:0 derivative 687.5033_10.748	687.5051 (100), 641.5032 (60), 255.232 (52)	Lipids and lipid-like molecules	3	C
73	RP-	10.808	693.4919	648.4937	[M + FA-H]-	n/a	FA 18:3;O derivative 693.4919_10.808	neg: 693.4897 (100), pos: 671.4852 (100; [M + Na]+), 317.2051 (10)	Lipids and lipid-like molecules	3	O
74	RP-	11.236	355.3206	310.3224	[M + FA-H]-	n/a	Unknown lipid 355.3206_11.236	309.3175 (100; [M-H]-), 55.0187 (61), 139.0680 (30), 115.0268 (19), 81.0899 (9)	Lipids and lipid-like molecules	4	D
75	RP-	11.265	677.4974	632.4992	[M + FA-H]-	n/a	FA 18:2;O derivative 677.4974_11.265	neg: 677.4942 (100), pos: 655.4904 (100; [M + Na]+), 319.2245 (7)	Lipids and lipid-like molecules	3	O
76	RP-	11.407	568.4929	569.5007	[M-H]-	n/a	Hydroxyhexadecanoic acid derivative	568.4939 (100), 225.2202 (25), 271.2280 (16)	Lipids and lipid-like molecules	3	O
77	HILIC+	0.812	316.2852	315.2770	[M + H]+	$C_{18}H_{37}NO_3$	Dehydrophytosphingosine	316.2852 (100), 280.2618 (16), 298.2760 (6), 60.0437 (5)	Organonitrogen compounds	2	A, B
78	HILIC+	0.952	207.1380	206.1302	[M + H]+	$C_{13}H_{18}O_2$	Unknown lipid 207.13803_0.952	95.0857 (100), 149.0962 (83), 207.1387 (54)	Lipids and lipid-like molecules	4	D
79	HILIC+	1.222	86.0969	85.0884	[M + H]+	$C_5H_{11}N$	Piperidine	86.0962 (100), 69.0701 (16)	Organoheterocyclic compounds	2	B

(*continued on next page*)

Table A1 (*continued*)

	ion mode	RT (min)	M_{obs}	M_{mi}	adduct	formula	annotation	*m/z* (intensity)*	compound classification	ID	ref
80	HILIC+	1.473	104.1080	104.1075	[M]+	$C_5H_{14}NO$	Choline	104.1069 (100), 60.0805 (12)	Organonitrogen compounds	1	A, B
81	HILIC+	1.529	321.2000	320.1921	[M + H]+	n/a	Choline derivative 321.2000_1.529	104.1068 (100), 60.0803 (24)	n/a	4	n/a
82	HILIC+	1.988	933.3691	466.1805	[2 M + H]+	n/a	Unknown glycosidic compound	489.1704 (100; [M + Na]+), 933.3842 (72; 2[M + Na]+), 467.1890 (57; [M + H]+);467.1898 (100), 241.0797 (73), 305.1354 (22)	n/a	4	n/a
83	HILIC+	1.995	473.1282	450.1390	[M + Na]+	n/a	Unknown 473.1282_1.995	473.1289 (100), 164.0309 (13)	n/a	4	n/a
84	HILIC+	3.533	257.1466	117.0800	[2 M + Na]+	$C_5H_{11}NO_2$	Betaine	140.0680 (100), 257.1465 (14)	Amino acids, peptides, and analogues	1	A, G
85	HILIC+	3.730	551.1953	528.2061	[M + Na]+	$C_{22}H_{32}N_4O_{11}$	Vicine + $C_{12}H_{16}O_4$	529.2123 (100), 143.0570 (30)	Carbohydrates and carbohydrate conjugates	3	K
86	HILIC+	3.979	297.0849	137.0478	[2 M + Na]+	$C_7H_7NO_2$	Trigonelline	160.0367 (100), 116.0569 (49)	Alkaloids and derivatives	1	A
87	HILIC+	4.081	690.3091	689.3013	[M + H]+	n/a	Unknown 690.3091_4.081	160.0371 (100), 573.1972 (14), 690.3082 (14), 141.0706 (11)	n/a	4	n/a
88	HILIC+	5.333	139.0978	138.0900	[M + H]+	n/a	Unknown 139.0978_5.333	139.0974 (100), 81.0453 (73), 83.0493 (58), 122.0702 (48), 93.0459 (38)	n/a	4	n/a
89	HILIC+	5.988	753.2796	752.2718	[M + H]+	n/a	Unknown 753.2796_5.988	753.2796 (100), 539.2060 (5), 227.1976 (3), 712.3908 (3)	n/a	4	n/a
90	HILIC+	6.097	344.0490	305.0858	[M + K]+	$C_{10}H_{15}N_3O_8$	Convicine	344.0483 (100); 144.0403 (100), 306.0912 (10; [M + H]+), 127.0400 (7)	Carbohydrates and carbohydrate conjugates	2	B, E
91	HILIC+	7.077	281.1275	280.1197	[M + H]+	n/a	Unknown 281.1275_7.077	88.0868 (100), 70.0659 (61), 281.1264 (44), 60.0441 (29), 236.0682 (23)	n/a	4	n/a
92	HILIC+	7.311	348.0710	347.0622	[M + H]+	$C_{10}H_{14}N_5O_7P$	Adenosine monophosphate	348.0716 (100), 136.0617 (98)	Nucleosides, nucleotides, and analogues	1	A, B
93	HILIC+	7.327	490.1274	467.1382	[M + Na]+	$C_{16}H_{25}N_3O_{13}$	Convicine hexose	144.0406 (100), 306.0939 (89), 468.1392 (17; [M + H]+); (490.1277; [M + Na]+)	Carbohydrates and carbohydrate conjugates	3	K
94	HILIC+	7.338	306.2136	305.2058	[M + H]+	n/a	Peptide	189.1340 (100; Val-Ala or Ala-Val), 118.0864 (35), 70.0864 (33), 116.0717 (13), 72.0803 (8) (306.2141; [M + H]-)	Amino acids, peptides, and analogues	3	N, R
95	HILIC+	7.655	365.0640	364.0561	[M + H]+	n/a	Unknown 365.0640_7.655	321.0735 (100), 365.0652 (100), 59.0493 (68), 194.0108 (62), 175.0304 (57), 148.0059 (48)	n/a	4	n/a
96	HILIC+	8.020	147.1127	146.1048	[M + H]+	$C_6H_{14}N_2O_2$	Lysine	84.0806 (100), 67.0537 (6), 55.0540 (5)	Amino acids, peptides, and analogues	1[‡]	A
97	HILIC+	8.165	540.7745	539.7667	[M + H]+	n/a	Unknown 540.7745_8.165	540.7746 (100), 532.2646 (24), 366.6928 (17)	n/a	4	n/a
98	HILIC+	8.187	285.1194	284.1115	[M + H]+	$C_{11}H_{16}N_4O_5$	Histidylglutamate	285.1199 (100), 267.1074 (80), 110.0729 (68)	Amino acids, peptides, and analogues	2	B, C

(*continued on next page*)

Table A1 (*continued*)

	ion mode	RT (min)	M_{obs}	M_{mi}	adduct	formula	annotation	*m/z* (intensity)*	compound classification	ID	ref
99	HILIC+	8.226	243.1086	242.1008	[M + H]+	$C_9H_{14}N_4O_4$	Histidylserine	83.0607 (100), 93.0438 (49), 110.0710 (22)	Amino acids, peptides, and analogues	2	A, B, C
100	HILIC+	9.414	180.0864	162.0526	[M + NH4]+	$C_6H_{13}NO_5$	Hydroxymethylglutaric acid	61.0277 (100); 85.0280 (100), 145.0491 (94), 127.0389 (45), 163.0593 (39; [M + H]+), 342.1386 (12; [2 M + NH4]+)	Lipids and lipid-like molecules	2	C
101	HILIC+	10.340	689.2109	688.2030	[M + H]+	n/a	Unknown 689.2109_10.340	689.2108 (100)	n/a	4	n/a
102	HILIC-	1.249	617.2408	504.2570	[M + 112.99-H]-	n/a	Unknown 617.2408_1.249	112.9856 (100), 617.2420 (53), 503.2497 (19; [M-H]-)	n/a	4	n/a
103	HILIC-	1.454	282.1553	283.1631	[M-H]-	$C_{12}H_{21}N_5O_3$	Histidyllysine	89.02397 (100)	Amino acids, peptides, and analogues	2	R
104	HILIC-	1.728	500.0571	387.0701	[M + 112.99-H]-	n/a	Unknown flavonoid 500.0571_1.728	224.0115 (100), 386.0628 (52), 180.0215 (37)	Phenylpropanoids and polyketides	4	H, I
105	HILIC-	3.054	130.9575	131.9654	[M + FA-H]-	n/a	Unknown 130.9575_3.054	117.6217 (100), 130.9557 (94), 125.0757 (74), 130.962 (58), 118.4721 (54)	n/a	4	n/a
106	HILIC-	4.981	611.2822	612.2900	[M-H]-	n/a	Unknown 611.2822_4.981	533.1317 (100), 552.8250 (98), 171.1026 (67), 600.8214 (65), 65.0155 (63)	n/a	4	n/a
107	HILIC-	5.233	739.1320	626.1435	[M + 112.99-H]-	n/a	Unknown 739.132_5.233	625.1362 (100; [M-H]-), 365.0378 (49)	n/a	4	n/a
108	HILIC-	6.186	727.1688	728.1766	[M-H]-	n/a	Unknown 727.1688_6.186	727.1677 (100)	n/a	4	n/a
109	HILIC-	6.205	699.1588	586.1748	[M + 112.99-H]-	n/a	Unknown 699.1588_6.205	585.1675 (100; [M-H]-), 699.1577 (77), 429.3351 (31), 83.0156 (29)	n/a	4	n/a
110	HILIC-	7.066	331.0248	196.0585	[M + 135.97-H]-	$C_6H_{12}O_7$	Gluconic or galactonic acid	195.0507 (100; [M-H]-), 331.0273 (36), 177.0394 (19)	Carbohydrates and carbohydrate conjugates	3	H
111	HILIC-	7.172	214.0482	215.0561	[M-H]-	n/a	Unknown 214.0482_7.172	214.0471 (100), 186.2744 (91), 176.8183 (88), 123.9246 (59), 202.9911 (45)	n/a	4	n/a
112	HILIC-	7.644	358.0548	359.0627	[M-H]-	n/a	Unknown 358.0548_7.644	314.0623 (100), 358.0563 (76), 196.0640 (65), 135.0440 (51)	n/a	4	n/a
113	HILIC-	7.715	461.1503	416.1536	[M + FA-H]-	n/a	Unknown 461.1503_7.715	179.0564 (100), 89.0242 (86), 324.0234 (77), 415.1463 (64), 235.0810 (34), 59.0146 (28)	n/a	4	n/a
114	HILIC-	8.166	566.1561	504.1682	[M + 64.00-2H]-	n/a	Trisaccharide	89.0236 (100), 503.1609 (99), 341.1102 (56), 179.0561 (36), 161.0483 (25)	Carbohydrates and carbohydrate conjugates	3	J
115	HILIC-	10.395	873.2712	828.2765	[M + FA-H]-	$C_{30}H_{52}O_{26}$	Verbascose	545.1684 100), 827.2692 (60), 383.1187 (48), 59.014 (22), 161.0444 (14), 179.0562 (9), 119.0332 (8), 221.0639 (4)	Carbohydrates and carbohydrate conjugates	1[‡]	G

RT, retention time; M_{obs}; observed mass; M_{mi}; monoisotopic mass; ID, Identification Level (1: standards of pure compounds, 2: MS/MS against public database, 3: mass or characterized chemical class, 4: unknown); ref., reference (A: Internal MS-Dial Library http://prime.psc.riken.jp/compms/msdial/main.html#MSP, B: FOODB https://foodb.ca/, C: HMDB https://hmdb.ca/, D: LIPID MAPS https://lipidmaps.org/, E: MS-Finder http://prime.psc.riken.jp/compms/msfinder/main.html, F:

ChEBI https://www.ebi.ac.uk/chebi/init.do, G: MoNA https://mona.fiehnlab.ucdavis.edu/, H: Fayek et al. (Fayek et al., 2021), I: Xia et al. (Xia et al., 2023), J: Abu-Reidah et al. (Abu-Reidah et al., 2014), K: Sergeant et al. (Sergeant et al., 2024), L: Pmhub https://pmhub.org.cn/, M: MassBank https://massbank.eu/MassBank/, N: *m/z* Cloud https://www.mzcloud.org/, O: Mecha et al. (Mecha et al., 2022), P: Lu et al. (Lu et al., 2022), Q: Nasciemento et al. (Nascimento et al., 2019), R: Koistinen et al. (Koistinen et al., 2018)). * The fragments reported were used for identification at ID level 1 and 2, while the most intense fragments were reported for ID levels 3 and 4. For some level 3 compounds, such as fatty acids, phospholipids, and vicine derivatives, certain characteristic fragments were specifically used to annotate the compound subclass. ǂ Compared to the standard, a systematic delay of approximately 1 min was observed in the HILIC retention time after around 7 min.

Appendix B. Supplementary data

Supplementary data to this article can be found online at https://doi.org/10.1016/j.foodchem.2025.143753.

Data availability

Data will be made available on request.

References

Abu-Reidah, I. M., del Mar Contreras, M., Arráez-Román, D., Fernández-Gutiérrez, A., & Segura-Carretero, A. (2014). UHPLC-ESI-QTOF-MS-based metabolic profiling of *Vicia faba* L. (Fabaceae) seeds as a key strategy for characterization in foodomics. *Electrophoresis, 35*(11), 1571–1581. https://doi.org/10.1002/elps.201300646

Akkad, R., Buchko, A., Johnston, S. P., Han, J., House, J. D., & Curtis, J. M. (2021). Sprouting improves the flavour quality of faba bean flours. *Food Chemistry, 364*, Article 130355. https://doi.org/10.1016/j.foodchem.2021.130355

Akkad, R., Kharraz, E., Han, J., House, J. D., & Curtis, J. M. (2019). Characterisation of the volatile flavour compounds in low and high tannin faba beans (*Vicia faba* var. minor) grown in Alberta, Canada. *Food Research International, 120*, 285–294. https://doi.org/10.1016/j.foodres.2019.02.044

Akkad, R., Kharraz, E., Han, J., House, J. D., & Curtis, J. M. (2022). The effect of short-term storage temperature on the key headspace volatile compounds observed in Canadian faba bean flour. *Food Science and Technology International, 28*(2), 135–143. https://doi.org/10.1177/1082013221998843

Amado, N. J., Hanselman, E. C., Harmon, C. P., Deng, D., Alarcon, S. M., Sharples, A. A., & Breslin, P. A. S. (2024). Ribonucleotides differentially modulate oral glutamate detection thresholds. *Chemical Senses, 49*, Article bjad049. https://doi.org/10.1093/chemse/bjad049

Augustin, M. A., & Cole, M. B. (2022). Towards a sustainable food system by design using faba bean protein as an example. *Trends in Food Science & Technology, 125*, 1–11. https://doi.org/10.1016/j.tifs.2022.04.029

Business Intelligence Consulting. (2023). *Market research reports*. https://www.factmr.com/.

Cevallos-Cevallos, J. M., Reyes-De-Corcuera, J. I., Etxeberria, E., Danyluk, M. D., & Rodrick, G. E. (2009). Metabolomic analysis in food science: A review. In Trends in food science and technology (Vol. 20, issues 11–12, pp. 557–566). doi:https://doi.org/10.1016/j.tifs.2009.07.002.

Chen, D.-W., Wan, P., Yao, J., Yang, X., & Liu, J. (2023). Egg yolk phospholipids as an ideal precursor of fatty note odorants for chicken meat and fried foods: A review. *Food Chemistry, 407*, Article 135177. https://doi.org/10.1016/j.foodchem.2022.135177

Dagan-Wiener, A., Di Pizio, A., Nissim, I., Bahia, M. S., Dubovski, N., Margulis, E., & Niv, M. Y. (2019). Bitterdb: Taste ligands and receptors database in 2019. *Nucleic Acids Research, 47*(D1), D1179–D1185. https://doi.org/10.1093/nar/gky974

Dhull, S. B., Kidwai Mohd, K., Noor, R., Chawla, P., & Rose, P. K. (2021). A review of nutritional profile and processing of faba bean (*Vicia faba* L.). *Legume Science*. https://doi.org/10.1002/leg3.129

Djoumbou Feunang, Y., Eisner, R., Knox, C., Chepelev, L., Hastings, J., Owen, G., … Wishart, D. S. (2016). ClassyFire: Automated chemical classification with a comprehensive, computable taxonomy. *Journal of Cheminformatics, 8*(1), 1–20. https://doi.org/10.1186/s13321-016-0174-y

Fayek, N. M., Mekky, R. H., Dias, C. N., Kropf, M., Heiss, A. G., Wessjohann, L. A., & Farag, M. A. (2021). UPLC-MS metabolome-based seed classification of 16 Vicia species: A Prospect for Phyto-equivalency and chemotaxonomy of different accessions. *Journal of Agricultural and Food Chemistry, 69*(17), 5252–5266. https://doi.org/10.1021/acs.jafc.0c06054

Ferrer-Gallego, R., Hernández-Hierro, J. M., Rivas-Gonzalo, J. C., & Escribano-Bailón, M. T. (2014). Sensory evaluation of bitterness and astringency sub-qualities of wine phenolic compounds: Synergistic effect and modulation by aromas. *Food Research International, 62*, 1100–1107. https://doi.org/10.1016/j.foodres.2014.05.049

Flores, F., Hybl, M., Knudsen, J. C., Marget, P., Muel, F., Nadal, S., … Rubiales, D. (2013). Adaptation of spring faba bean types across European climates. *Field Crops Research, 145*, 1–9. https://doi.org/10.1016/j.fcr.2013.01.022

Foyer, C. H., Lam, H. M., Nguyen, H. T., Siddique, K. H. M., Varshney, R. K., Colmer, T. D., … Considine, M. J. (2016). Neglecting legumes has compromised human health and sustainable food production. *Nature Plants, 2*(8). https://doi.org/10.1038/NPLANTS.2016.112

Gläser, P., Mittermeier-Kleßinger, V. K., Spaccasassi, A., Hofmann, T., & Dawid, C. (2021). Quantification and bitter taste contribution of lipids and their oxidation products in pea-protein isolates (*Pisum sativum* L.). *Journal of Agricultural and Food Chemistry, 69*(31), 8768–8776. https://doi.org/10.1021/acs.jafc.1c02889

He, L., Hu, Q., Wei, L., Ge, X., Yu, N., & Chen, Y. (2023). Unravelling dynamic changes in non-volatile and volatile metabolites of pulses during soaking: An integrated metabolomics approach. *Food Chemistry, 422*. https://doi.org/10.1016/j.foodchem.2023.136231

Hefni, M., McEntyre, C., Lever, M., & Slow, S. (2015). A simple HPLC method with fluorescence detection for choline quantification in foods. *Food Analytical Methods, 8*(9), 2401–2408. https://doi.org/10.1007/s12161-015-0131-9

Inci, N. E., & Toker, C. (2011). Screening and selection of faba beans (*Vicia faba* L.) for cold tolerance and comparison to wild relatives. *Genetic Resources and Crop Evolution, 58*(8), 1169–1175. https://doi.org/10.1007/S10722-010-9649-2

Jeganathan, B., Vasanthan, T., & Temelli, F. (2023). Isolation of clean-label faba bean (*Vicia faba* L.) proteins: A comparative study of mild fractionation methods against traditional technologies. *Innovative Food Science and Emerging Technologies, 84*. https://doi.org/10.1016/j.ifset.2023.103285

Karolkowski, A., Belloir, C., Briand, L., & Salles, C. (2023). Non-volatile compounds involved in bitterness and astringency of pulses: A review. In *Molecules* (Vol. 28, issue 8). MDPI. doi:https://doi.org/10.3390/molecules28083298.

Karolkowski, A., Belloir, C., Lucchi, G., Martin, C., Bouzidi, E., Levavasseur, L., Salles, C., & Briand, L. (2023). Activation of bitter taste receptors by saponins and alkaloids identified in faba beans (*Vicia faba L. minor*). *Food Chemistry, 426*, Article 136548. https://doi.org/10.1016/j.foodchem.2023.136548

Karolkowski, A., Martin, C., Bouzidi, E., Albouy, J.-F., Levavasseur, L., Briand, L., & Salles, C. (2022). Heat treatment, cultivar and formulation modify the sensory properties and consumer acceptability of gels containing Faba bean (*Vicia faba L. minor*) protein concentrates. *Foods, 11*(19). https://doi.org/10.3390/foods11193018

Karolkowski, A., Meudec, E., Bruguière, A., Mitaine-Offer, A. C., Bouzidi, E., Levavasseur, L., … Salles, C. (2023). Faba bean (*Vicia faba L. minor*) bitterness: An untargeted Metabolomic approach to highlight the impact of the non-volatile fraction. *Metabolites, 13*(8). https://doi.org/10.3390/metabo13080964

Klåvus, A., Kokla, M., Noerman, S., Koistinen, V. M., Tuomainen, M., Zarei, I., … Hanhineva, K. (2020). "Notame": Workflow for non-targeted LC–MS metabolic profiling. *Metabolites, 10*(4). https://doi.org/10.3390/metabo10040135

Koc, F. N., & Dinler, B. S. (2022). Pipecolic acid in plants: Biosynthesis, signalling, and role under stress. *Botanica Lithuanica, 28*(1).

Koistinen, V. M., Mattila, O., Katina, K., Poutanen, K., Aura, A.-M., & Hanhineva, K. (2018). Metabolic profiling of sourdough fermented wheat and rye bread. *Scientific Reports, 8*(1), 5684.

Kumari, S., Memba, L. J., Dahuja, A., Vinutha, T., Saha, S., & Sachdev, A. (2016). Elucidation of the role of oleosin in off-flavour generation in soymeal through supercritical CO2 and biotic elicitor treatments. *Food Chemistry, 205*, 264–271. https://doi.org/10.1016/j.foodchem.2016.03.028

Lu, A., Cao, J., Gang, L., Tan, D. P., Qin, L., Lu, Y. L., … He, Y. Q. (2022). UPLC-Q/TOF-MS coupled with multivariate analysis for comparative analysis of metabolomic in Dendrobium nobile from different growth altitudes. *Arabian Journal of Chemistry, 15*(11). https://doi.org/10.1016/j.arabjc.2022.104208

Luzzatto, L., & Arese, P. (2018). Favism and Glucose-6-phosphate dehydrogenase deficiency. *New England Journal of Medicine, 378*(1), 60–71. https://doi.org/10.1056/NEJMra1708111

Mecha, E., Erny, G. L., Guerreiro, A. C. L., Feliciano, R. P., Barbosa, I., Bento da Silva, A., … Bronze, M. R. (2022). Metabolomics profile responses to changing environments in a common bean (*Phaseolus vulgaris* L.) germplasm collection. *Food Chemistry, 370*. https://doi.org/10.1016/j.foodchem.2021.131003

Medawar, E., Huhn, S., Villringer, A., & Veronica Witte, A. (2019). The effects of plant-based diets on the body and the brain: A systematic review. In *, Vol. 9. Translational psychiatry*. Nature Publishing Group. https://doi.org/10.1038/s41398-019-0552-0, 1.

Mekky, R. H., Thabet, M. M., Rodríguez-Pérez, C., Elnaggar, D. M. Y., Mahrous, E. A., Segura-Carretero, A., & Abdel-Sattar, E. (2020). Comparative metabolite profiling and antioxidant potentials of seeds and sprouts of three Egyptian cultivars of *Vicia faba* L. *Food Research International, 136*. https://doi.org/10.1016/j.foodres.2020.109537

Menis-Henrique, M. E. C. (2020). Methodologies to advance the understanding of flavor chemistry. In *, Vol. 33. Current opinion in food science* (pp. 131–135). Elsevier Ltd.. https://doi.org/10.1016/j.cofs.2020.04.005

Meyerhof, W., Batram, C., Kuhn, C., Brockhoff, A., Chudoba, E., Bufe, B., Appendino, G., & Behrens, M. (2010). The molecular receptive ranges of human TAS2R bitter taste receptors. *Chemical Senses, 35*(2), 157–170.

Mohan, N., & Mellem, J. J. (2020). Functional properties of the protein isolates of hyacinth bean [*Lablab purpureus* (L.) sweet]: An effect of the used procedures. *LWT, 129*. https://doi.org/10.1016/j.lwt.2020.109572

Morelli, C. F., Pappalardo, V., Brockhoff, A., Pieraccini, S., Sironi, M., Sangiorgio, S., … Rabuffetti, M. (2022). Purine 5′-ribonucleotide-l-glutamate hybrids as potential tools to investigate the mechanism of umami taste reception. *ChemistrySelect, 7*(45), Article e202204123. https://doi.org/10.1002/slct.202204123

Nascimento, Y. M., Abreu, L. S., Lima, R. L., Costa, V. C. O., De Melo, J. I. M., Braz-Filho, R., … Tavares, J. F. (2019). Rapid characterization of triterpene Saponins from *Zornia brasiliensis* by HPLC-ESI-MS/MS. *Molecules, 24*(14). https://doi.org/10.3390/molecules24142519

Pasqualone, A., Abdallah, A., & Summo, C. (2020). Symbolic meaning and use of broad beans in traditional foods of the Mediterranean Basin and the Middle East. *Journal of Ethnic Foods, 7*(39), 1–13. https://doi.org/10.1186/s42779-020-00073-1

Roland, W. S. U., Pouvreau, L., Curran, J., van de Velde, F., & de Kok, P. M. T. (2017). Flavor aspects of pulse ingredients. *Cereal Chemistry, 94*(1), 58–65. https://doi.org/10.1094/CCHEM-06-16-0161-FI

Sergeant, K., Goertz, S., Halime, S., Tietgen, H., Heidt, H., Minestrini, M., … Renaut, J. (2024). Exploration of the diversity of Vicine and Convicine derivatives in Faba bean (*Vicia faba* L.) cultivars: Insights from LC-MS/MS spectra. *Molecules, 29*(5). https://doi.org/10.3390/molecules29051065

Shiga, K., Yamamoto, S., Nakajima, A., Kodama, Y., Imamura, M., Sato, T., Uchida, R., Obata, A., Bamba, T., & Fukusaki, E. (2014). Metabolic profiling approach to explore compounds related to the umami intensity of soy sauce. *Journal of Agricultural and Food Chemistry, 62*(29), 7317–7322. https://doi.org/10.1021/jf501173r

Sonntag, T., Kunert, C., Dunkel, A., & Hofmann, T. (2010). Sensory-guided identification of N-(1-Methyl-4-oxoimidazolidin-2-ylidene)- α-amino acids as contributors to the thick-sour and mouth-drying orosensation of stewed beef juice. *Journal of Agricultural and Food Chemistry, 58*(10), 6341–6350. https://doi.org/10.1021/jf100591c

Spaggiari, G., Di Pizio, A., & Cozzini, P. (2020). Sweet, umami and bitter taste receptors: State of the art of in silico molecular modeling approaches. In *, Vol. 96. Trends in food science and technology* (pp. 21–29). Elsevier Ltd.. https://doi.org/10.1016/j.tifs.2019.12.002

Sumner, L. W., Amberg, A., Barrett, D., Beale, M. H., Beger, R., Daykin, C. A., … Griffin, J. L. (2007). Proposed minimum reporting standards for chemical analysis: Chemical analysis working group (CAWG) metabolomics standards initiative (MSI). *Metabolomics, 3*, 211–221.

Tuccillo, F., Kantanen, K., Wang, Y., Martin Ramos Diaz, J., Pulkkinen, M., Edelmann, M., Knaapila, A., Jouppila, K., Piironen, V., Lampi, A.-M., Sandell, M., & Katina, K. (2022). The flavor of faba bean ingredients and extrudates: Chemical and sensory properties. *Food Research International, 162*, Article 112036. https://doi.org/10.1016/j.foodres.2022.112036

Tuccillo, F., Lampi, A.-M., Katina, K., & Sandell, M. (2024). Exploring the lack of liking for faba bean ingredients with different sensory profiles. *Food Quality and Preference, 118*, Article 105198. https://doi.org/10.1016/j.foodqual.2024.105198

Tuccillo, F., Wang, Y., Edelmann, M., Lampi, A. M., Coda, R., & Katina, K. (2022). Fermentation conditions affect the synthesis of volatile compounds, dextran, and organic acids by *Weissella confusa* A16 in Faba bean protein concentrate. *Foods, 11*(22), 3579. https://doi.org/10.3390/FOODS11223579/S1

Valente, I. M., Cabrita, A. R. J., Malushi, N., Oliveira, H. M., Papa, L., Rodrigues, J. A., … Maia, M. R. G. (2019). Unravelling the phytonutrients and antioxidant properties of European *Vicia faba* L. seeds. *Food Research International, 116*, 888–896. https://doi.org/10.1016/j.foodres.2018.09.025

Valente, I. M., Maia, M. R. G., Malushi, N., Oliveira, H. M., Papa, L., Rodrigues, J. A., … Cabrita, A. R. J. (2018). Profiling of phenolic compounds and antioxidant properties of European varieties and cultivars of *Vicia faba* L. pods. *Phytochemistry, 152*, 223–229. https://doi.org/10.1016/j.phytochem.2018.05.011

Vogelsang-O'Dwyer, M., Petersen, I. L., Joehnke, M. S., Sørensen, J. C., Bez, J., Detzel, A., … Zannini, E. (2020). Comparison of Faba bean protein ingredients produced using dry fractionation and isoelectric precipitation: Techno-functional, nutritional and environmental performance. *Foods, 9*(3). https://doi.org/10.3390/foods9030322

Wang, Y., Tuccillo, F., Lampi, A., Knaapila, A., Pulkkinen, M., Kariluoto, S., Coda, R., Edelmann, M., Jouppila, K., Sandell, M., Piironen, V., & Katina, K. (2022). Flavor challenges in extruded plant-based meat alternatives: A review. *Comprehensive Reviews in Food Science and Food Safety*. https://doi.org/10.1111/1541-4337.12964

Wang, Y., Tuccillo, F., Niklander, K., Livi, G., Siitonen, A., Pöri, P., … Katina, K. (2024). Masking off-flavors of faba bean protein concentrate and extrudate: The role of in situ and in vitro produced dextran. *Food Hydrocolloids, 150*, Article 109692. https://doi.org/10.1016/j.foodhyd.2023.109692

Wang, Y., Zhao, P., Zhou, Y., Hu, X., & Xiong, H. (2023). From bitter to delicious: Properties and uses of microbial aminopeptidases. *World Journal of Microbiology and Biotechnology, 39*(3), 72.

Wishart, D. S. (2008). Metabolomics: Applications to food science and nutrition research. In Trends in food science and technology (Vol. 19, issue 9, pp. 482–493). doi:https://doi.org/10.1016/j.tifs.2008.03.003.

Xia, M., Li, M., de Souza, T. S. P., Barrow, C., Dunshea, F. R., & Suleria, H. A. R. (2023). LC-ESI-QTOF-MS2 characterization of phenolic compounds in different lentil (*Lens culinaris* M.) samples and their antioxidant capacity. *Frontiers in Bioscience - Landmark, 28*(3). https://doi.org/10.31083/j.fbl2803044

Yan, J., & Tong, H. (2023). An overview of bitter compounds in foodstuffs: Classifications, evaluation methods for sensory contribution, separation and identification techniques, and mechanism of bitter taste transduction. *Comprehensive Reviews in Food Science and Food Safety, 22*(1), 187–232. https://doi.org/10.1111/1541-4337.13067

Zeisel, S. H., & Da Costa, K. A. (2009). Choline: An essential nutrient for public health. In Nutrition reviews (Vol. 67, issue 11, pp. 615–623). doi:https://doi.org/10.1111/j.1753-4887.2009.00246.x.

Zhang, Y., Zhu, Y., Zhao, N., Wu, J., & Hu, Y. (2016). Application of isothermal titration calorimeter for screening bitterness-suppressing molecules of quinine. *Food Chemistry, 190*, 1007–1012. https://doi.org/10.1016/j.foodchem.2015.06.070

Ziaikin, E., Tello, E., Peterson, D. G., & Niv, M. Y. (2023). BitterMasS: Predicting bitterness from mass spectra. *Journal of Agricultural and Food Chemistry*. https://doi.org/10.1021/acs.jafc.3c09767